

**UNIVERSITY OF TURKISH AERONAUTICAL ASSOCIATION
INSTITUTE OF SCIENCE AND TECHNOLOGY**

**CSC-STATCOM CONTROL TO COMPENSATE
REACTIVE POWER UNDER DISTURBANCE
CONDITIONS OF POWER SYSTEM**



MASTER THESIS

Mahmood ABED

**THE DEPARTMENT OF ELECTRICAL AND ELECTRONIC
ENGINEERING**

THE PROGRAM OF ELECTRICAL AND ELECTRONIC ENGINEERING

SEPTEMBER 2017

**UNIVERSITY OF TURKISH AERONAUTICAL ASSOCIATION
INSTITUTE OF SCIENCE AND TECHNOLOGY**

**CSC-STATCOM CONTROL TO COMPENSATE
REACTIVE POWER UNDER DISTURBANCE
CONDITIONS OF POWER SYSTEM**



MASTER THESIS

Mahmood ABED

1406030026

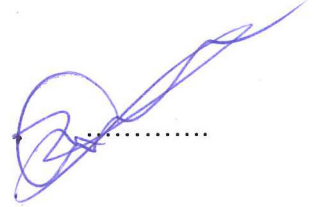
**THE DEPARTMENT OF ELECTRICAL AND ELECTRONIC
ENGINEERING**

THE PROGRAM OF ELECTRICAL AND ELECTRONIC ENGINEERING

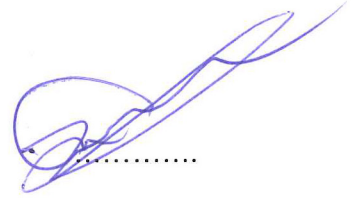
Supervisor: Prof. Dr. Dođan ÇALIKOĐLU

Mahmood Abed, having student number 1406030026 and enrolled in the Master Program at the Institute of Science and Technology at the University of Turkish Aeronautical Association, after meeting all of the required conditions contained in the related regulations, has successfully accomplished, in front of the jury, the presentation of the thesis prepared with the title of: “CSC-Statcom Control to Compensate Reactive Power Under Disturbance Conditions of Power System”

Supervisor : Prof. Dr. Dođan ALIKOĐLU
University of Turkish Aeronautical Association



Jury Members : Prof. Dr. Dođan ALIKOĐLU
University of Turkish Aeronautical Association



: Assoc. Prof. Dr. Ahmet KARAARSLAN
Ankara Yıldırım Beyazıt University



: Assist. Prof. Dr. Ibrahim MAHARIQ
The University of Turkish Aeronautical Association



Thesis Defense Date: 21 September 2017

**UNIVERSITY OF TURKISH AERONAUTICAL ASSOCIATION
INSTITUTE OF SCIENCE AND TECHNOLOGY**

I hereby declare that all the information in this study I presented as my Master's Thesis, called: "CSC-Statcom Control to Compensate Reactive Power Under Disturbance Conditions of Power System" has been presented in accordance with the academic rules and ethical conduct. I also declare and certify with my honor that I have fully cited and referenced all the sources I made use of in this present study.



21.09.2017

Mahmood ABED

To My Parents



ACKNOWLEDGMENTS

First and foremost, I would like to give thanks and praise to the Almighty God for His grace and blessings throughout the entire project. without Him, this is nothing.

I would like to express my deepest thanks and gratitude to my supervisor Prof. Dr. Doğan ÇALIKOĞLU for his guidance, encouragement, valuable advice and thought provoking ideas that had helped me in this thesis work. I am also thankful to the staff members, faculty of the Department of the Electrical and Electronic Engineering/THK. I would also like to extend my appreciation to my committee members for their participation in this thesis. I would also like to thank my parents, my brothers, my sisters and my friends for giving me the necessary impetus towards the development of this thesis work. Finally, I would like to thank all the people those I work with and they helped me in my life.

September 2017

Mahmood ABED

TABLE OF CONTENTS

ACKNOWLEDGMENTS	v
TABLE OF CONTENTS	vi
LIST OF FIGURES	vii
ABBREVIATIONS AND NOMENCLATURE.....	ix
ABSTRACT.....	x
ÖZET	xii
CHAPTER ONE	1
1. INTRODUCTION	1
1.1 Presentation of The Work.....	1
1.2 Overview of Power System Disturbances	2
1.3 Static Synchronous Compensator (STATCOM)	3
1.3.1 The Importance of (STATCOM) and Its Applications	4
1.3.2 The Types of (STATCOM) and Its Varies Properties.....	5
1.4 Literature Survey	6
1.5 Significance of The Study	8
1.6 Organization of the Dissertation.....	9
CHAPTER TWO	10
2. SYSTEM DESCRIPTION AND OPERATING PRINCIPLES OF CURRENT SOURCE CONVERTER BASED STATCOM	10
2.1 Introduction.....	10
2.2 Basic Circuit Arrangement	10
2.3 Principles of Reactive Power Control.....	12
2.4 Pulse Width Modulation Techniques.....	20
CHAPTER THREE	27
3. REACTIVE POWER CONTROL METHOD FOR CURRENT SOURCE CONVERTER BASED STATCOM	27
3.1 Conventional Control Method based on PI Controller	27
3.2 Modern Control Method based on State Feedback-Controller and pole placement controller	30
CHAPTER FOUR	37
4. SIMULATION AND DISCUSSION OF RESULTS	37
4.1 Simulation Circuit	37
CHAPTER FIVE	49
5. CONCLUSIONS AND SUGGESTIONS FOR FUTURE WORK	49
5.1 Conclusions	49
5.2 Future work	49
REFERENCES	51
APPENDIX	55
Appendix A: Modeling of Current Source Converter Based Statcom in DQ Stationary Frame	56
Appendix-B: Calculations of K, J and N matrices	64
CURRICULUM VITAE	67

LIST OF FIGURES

Figure 2.1	: Topology of three phase current source converter for general circuit.	11
Figure 2.2	: CSC Circuit diagram without input filter.	12
Figure 2.3	: Switching signals of S1&S2, and the corresponding theoretical converter input current, $i_R(t)$ and line-to-line voltage, $v_{ST}(t)$ for inductive reactive power.	13
Figure 2.4	: Principle phasor diagram of CSC in a steady-state (a) for inductive (b) capacitive reactive power generation.	14
Figure 2.5	: Switching signals of S1&S2, and the corresponding theoretical converter input current, $i_R(t)$ and line-to-line voltage, $v_{ST}(t)$ for capacitive reactive power generation of CSC.	15
Figure 2.6	: Theoretical active and reactive power variations of CSC STATCOM w.r.t. angle, θ at a fixed modulation index.	17
Figure 2.7	: Phasor diagram of CSC in a lossless system (transient-state representation) for inductive (b) capacitive reactive power generation.	18
Figure 2.8	: Phasor diagram of CSC in a lossless system (steady-state representation) (a)for inductive (b)capacitive reactive power generation.	18
Figure 2.9	: Equivalent single line diagram of CSC based STATCOM.	19
Figure 2.10	: Illustration of variations in converter input voltage, VCR with the generated reactive power of CSC.	19
Figure 2.11	: Typical switching patterns for MSPWM ($M=0.5, f_{carrier}=1200\text{Hz}$).	21
Figure 2.12	: Typical switching patterns for SVPWM ($M= 0.5, f_{carrier}=1200\text{Hz}$).	22
Figure 2.13	: Typical switching patterns for SHEM (elimination of 5th, 7th, 11th and 13th harmonics at $M=0.8$).	23
Figure 2.14	: Normalized harmonic spectra of converter input current w.r.t. dc-link current (a) for MSPWM (b) for SVPWM (c) for SHEM.	24
Figure 2.15	: Normalized harmonic spectra of converter input current w.r.t. dc-link current (a) for MSPWM (b) for SVPWM when carrier frequency, $f_{carrier}= 3\text{kHz}$	26
Figure 3.1	: Control system based conventional PI controller.	28
Figure 3.2	: Control system based conventional PI controller for CSC based STATCOM, where modulation index control is not applicable.	28

Figure 3.3	: Steps applied in tuning PI parameters of CSC based STATCOM control system (a) for dc-link current controller, and (b) for reactive power controller.....	29
Figure 3.4	: Equivalent circuit of CSC based STATCOM in abc-rotating frame.....	30
Figure 3.5	: Equivalent circuit of CSC based STATCOM in dq-stationary frame (a) for steady-state, (b) for transient-state.....	31
Figure 3.6	: Typical block diagram of modern control method based on state feedback controller for CSC based STATCOM.	33
Figure 3.7	: Control structure of pole placement controller based CSC-STATCOM.....	36
Figure 4.1	: Simulation circuit with CSC-STATCOM connected to 2 sources 3 buses system test.....	38
Figure 4.2	: Subsystem of Pole Shifting Controller Based CSC-STATCOM.....	39
Figure 4.3	: Bus voltages in p.u w.r.t. time without CSC-STATCOM and with CSC-STATCOM for the first case.....	40
Figure 4.4	: Active power of CSC-STATCOM in MW w.r.t. time for the first case.....	42
Figure 4.5	: Reactive power of CSC-STATCOM in MVAR w.r.t. time for the first case.....	42
Figure 4.6	: Bus voltages in p.u w.r.t. time without CSC-STATCOM for the second case.....	43
Figure 4.7	: Bus voltage in p.u w.r.t. time with CSC-STATCOM for the second case.....	44
Figure 4.8	: Active power of CSC-STATCOM in MW w.r.t. time for the second case.....	45
Figure 4.9	: Reactive power of CSC-STATCOM in MVAR w.r.t. time for the second case.....	45
Figure 4.10	: Bus voltages in p.u w.r.t. time without CSC-STATCOM and with CSC- STATCOM for the third case.....	46
Figure 4.11	: Active power of CSC-STATCOM in MW w.r.t. time for the third case.....	47
Figure 4.12	: Reactive power of CSC-STATCOM in MVAR w.r.t. time for the third case.....	48

ABBREVIATIONS AND NOMENCLATURE

CSC	: Current Source Converter
VSC	: Voltage Source Converter
PWM	: Pulse Width Modulation
SPWM	: Sinusoidal PWM
SVPWM	: Space Vector PWM
MSPWM	: Modified Sinusoidal PWM
SHEM	: Selective Harmonic Elimination Method
IGCT	: Integrated Gate Commutated Thyristor
HV IGBT	: High Voltage Integrated Gate Bipolar
Transistor GTO	: Gate Turn-Off Thyristor
SCR	: Silicon Controlled Rectifier
FACTS	: Flexible AC Transmission
Systems AC	: Alternating Current
DC	: Direct Current
STATCOM	: Static Synchronous Compensator
D-STATCOM	: Distribution type STATCOM
TSC	: Thyristor Switched Capacitor
TCR	: Thyristor Controlled Reactor
SVC	: Static VAR Compensator
VA	: Volt-Ampere
VAR (r)	: Volt-Ampere Reactive
M	: modulation index
θ	: phase angle between line-to-line voltage and the other line current
\emptyset	: phase shift angle defined as θ rads in inductive mode and $(\pi - \theta)$ rads in capacitive mode of operation of CSC STATCOM
F_s	: switching frequency of power semiconductors
f_1	: fundamental frequency, which is also the frequency of power system (i.e., 50Hz)
f_{carrier}	: frequency of carrier signal in PWM applications
f_c	: corner frequency of low pass input filter
I_{dc}	: mean value of dc-link current
L_{dc}	: inductance of dc-link reactor in CSC STATCOM
R_{dc}	: internal resistance of dc-link reactor in CSCSTATCOM
IR1	: magnitude of fundamental-frequency component of converter line current in phase R

ABSTRACT

CSC-STATCOM CONTROL TO COMPENSATE REACTIVE POWER UNDER DISTURBANCE CONDITIONS OF POWER SYSTEM

ABED, Mahmood

Master, Department of Electrical and Electronics Engineering

Supervisor: Prof. Dr. Doğan ÇALIKOĞLU

September 2017, 67 pages

Enhancing the quality of power system by injecting or absorbing reactive power by using Current Source Converter based Static Synchronous Compensator is investigated in this thesis. It is a shunt flexible alternative current transmission system instrument, which has important function as a stability bolster for disturbances due to the sudden connection of heavy inductive load. This research work brings forth the influence of (CSC-STATCOM) based controlled for improving power quality of power system under heavy inductive loads disturbance cases. The proposed method employs CSC based STATCOM to inject reactive power in the system to preserve the stability of the bus voltages in high emergency condition. The control of reactive power is obtained by applying the pole-shifting control method with considering modulation index variables as inputs and the variables (dc link current and quadrant component AC side current component) as output variables to get better response. Firstly, CSC-STATCOM circuit is analyzed. Secondly, its differential equations are transferred from abc rotating frame to $0dq$ stationary frame to get the final state-space representation. Then, pole-shifting controller for CSC based STATCOM is analyzed based on this state-space representation. After that, the influence of the proposed method in the two sources power system circuit with three phase fault and sudden connection of high inductive

loads is investigated. Here, pertinence of the proposed method is achieved by MATLAB simulation and the results show an improvement in the quality of power system by using CSC-STATCOM.

Keywords: power quality, reactive power compensation, pole-shifting controller, Current source converter, STATCOM, heavy inductive load, disturbances.



ÖZET

GÜÇ SİSTEMİ BOZULMA KOŞULLARI ALTINDAYKEN REAKTİF GÜCÜ DENGELERMEK İÇİN AKD-STATKOM KONTROLÜ

ABED, Mahmood

Yüksek Lisans, Elektrik ve Elektronik Mühendisliği

Tez Danışmanı: Prf. Dr. Doğan ÇALIKOĞLU

Eylül 2017, 67 sayfa

Bu tez çalışmasında, Akım Kaynak Dönüştürücü tabanlı Statik Senkron Kompansatör kullanarak reaktif gücü absorbe ederek veya enjekte ederek güç sisteminin kalitesini artırma konusu araştırılmaktadır. Bu bir paralel esnek alternatif akım iletim sistemi elemanı olup, ani ağır endüktif yük bağlantısı nedeniyle oluşan bozulmalar için istikrar desteği olarak önemli bir işleve sahiptir. Bu çalışma, ağır endüktif yük bozulma durumlarında elektrik sisteminin güç kalitesini artırmak için (AKD-STATKOM) kontrolünün etkisini öne çıkarmayı amaçlamaktadır. Önerilen yöntemde, AKD tabanlı STATKOM acil durumlar karşısında bara voltajını korumak için sistemde reaktif güç enjekte etmek için kullanılmaktadır. Reaktif gücün kontrolü daha iyi yanıt elde etmek için girdi olarak modülasyon katsayısı değişkenlerini göz önünde bulundurarak kutup değiştirme kontrol metodunun uygulanması ile (DA bağlantı akımı ve kuadrant bileşeni AA yan akım elemanı) gibi değişkenleri çıktı değişkenleri olarak uygulayarak sağlanır. İlk olarak, AKD-STATKOM devresi edilmektedir. İkinci olarak, nihai durum-uzay temsili elde etmek için diferansiyel denklemleri abc dönen çerçeveden $0dq$ hareketsiz çerçeveye aktarılmaktadır. Daha sonra AKD tabanlı STATKOM için kutup değiştiren kontrolör bu durum-uzay temsiline dayanılarak analiz edilmektedir. Bundan sonra üç fazlı iki kaynaklı güç sistemi devresinde önerilen yöntemin etkisi ve yüksek endüktif yükün ani bağlantısı araştırılmaktadır. Burada önerilen yöntemin geçerliliği ve uygunluğu

MATLAB simülasyonu ile elde edilmiş olup, sonuçlar AKD-STATKOM kullanılarak güç sisteminin kalitesinde bir iyileşme sağlandığı göstermektedir.

Anahtar Kelimeler: güç kalitesi, reaktif güç dengeleme, kutup değıştiren kontrolör, akım kaynak dönüştürücü, STATKOM, ağır endüktif yük, bozulmalar



CHAPTER ONE

INTRODUCTION

1.1 Presentation of The Work

In this work, how to improve the power quality in transmission systems by compensating the reactive power in the power system in heavy inductive load case is investigated. The utilization of CSC-STATCOM is chosen for this purpose. Its operation mode depends on the increase of inductive or capacitive characteristics in the power system. This work employs pole shifting controller based CSC-STATCOM for this purpose. It consists of three phase bridge converter with six power electronic switches. The DC side is connected with energy storage (inductor) and equivalent series resistor. The AC output of this converter is linked with capacitive filter. It is one of Facts types that is connected with any bus in a power system as shunt connection through a coupling transformer. The voltage of any bus in power system can be represented by p.u value. This STATCOM component works to fix voltage value at 1 p.u at disturbance conditions. In the beginning, a power system circuit with two voltage sources is simulated with sudden connection of two heavy inductive loads (50MW-30MVAR) and (100MW and 50MVAR) respectively at different periods. After that, pole shifting controller based CSC-STATCOM is used to inject the required capacitive reactive power. This controller has been utilized after transforming the differential equations of CSC-STATCOM from abc rotating frame to $0dq$ stationary frame. This is in order to decrease the number of state variables and make them dc quantities in steady-state to obtain the state-space representation of the STATCOM. The feedback gain matrix of pole shifting controller is calculated based on the desired poles position.

1.2 Overview of Power System Disturbances

Until last years, the fundamental interest of buyers in power system was the validity of source which is known as the continuousness of energy. It is not only the continuity that consumers need these days, they seek to quality of electricity source also. The electric power quality, approximately denotes to keeping up an almost sinusoidal bus voltage at constant level in magnitude and frequency in continual way. For generating plant that produces voltages nearly completely sinusoidal at rated value and frequency, power quality problems begin with transmission system and remain effective until arrive users in distribution system. In the terms, describing the disturbances in the power system have been explained as follows [1,2]:

a) Transients: are defined as the variation in a system variable that decays during transformation from one steady-state operating state to another and can be characterized as impulsive transients and oscillatory transients. Impulse transients are generally produced when the transmission lines expose to lightning strikes. The capacitor or transformer energization and converter switching cause oscillatory transients. While impulsive transient is a speedy with a fast rise and decaying time, oscillatory transient includes one or more sinusoidal components with frequencies in the range from power frequency to 500kHz and decays in time.

b) Short duration voltage variations: The faults, login of large loads and speedily varying large reactive power demands of loads cause variations in supply voltage for one minute as maximum period. These are called as voltage swells, interruption and voltage sags.

c) Long duration voltage variations: The switching off (or on) causes rms value for the supply voltage to vary more than one minute at fundamental frequency like overvoltage (or under voltage).

d) Voltage unbalance: The single phase loads cause changing in the magnitude of three phase voltages of the electric source and may be difference shifting between them with respect to time

e) Waveform distortion: It happens when the voltage or current waveform deflects than perfect sinusoidal at steady-state condition. The types of these distortions are notching, dc-offset and harmonics. The geomagnetic disturbances in power system produce dc-offsets, essentially at half-wave rectifications and

maximum altitudes. These will result in increasing of heat in the transformer because of high peak value of the flux in the transformer that leads to saturation. The harmonics in the power systems are produced by power electronics. The operation of power converters result in a periodic voltage distortion (notching) current transfer from one phase to another one.

f) Fluctuations of voltage: It is found when the power system includes low power factor loads such as arc furnaces. These loads cause high variations in the magnitude of drawn currents and random changing in voltage of the supply and that is called Fluctuation or “Voltage Flicker”.

g) Power frequency variations: The fast changes in the load that connected to low inertia system such as the operation of draglines produces variations in power Frequency. These variations cause negative effect on the life span of turbine blades for generation plant

All of these cases above are kinds of disturbances or transients obtain in power system and effect on power quality. The increasing stability limits of transmission lines and the capability of loading are achieved from the engineers point of view by control flow of active and reactive powers with utilizing power electronic based power conditioning devices for compensating cases to improve power quality.

1.3 Static Synchronous Compensator (STATCOM)

According to definition of IEEE PES task force of facts working group: *Static Synchronous Compensator (STATCOM)*: A static synchronous generator functions as a shunt-connected compensator for reactive power by controlling output current independently than the voltage of the system. This output current is inductive or capacitive current.

In 1976, Gyugi discovered the ability to produce reactive power based controlled without utilizing switching power converters which control on the output of energy stored in capacitors and reactors [3]. The operation of reactive power production from the standpoint of view is like to that of a perfect synchronous machine. The excitation control is responsible of changing the reactive power output of the synchronous machine control. The converters can exchange real power with the ac system like this mechanical machine if it is connected to a suitable dc energy supply. They are named Static Synchronous Generator (SSG) because of these

symmetries with a rotating synchronous generator. If SSG is operated as shunt-connected reactive compensator with suitable controls without energy supply, it is called a Static Synchronous Compensator (STATCOM). It is similar to the rotating synchronous compensator (condenser).

The electrical engineers used rotating synchronous condensers (RSC) in transmission and distribution systems for 60 years. Today, their using decreased significantly because of the following points: i) need an important amount of protective and starting instruments and significant establishments, ii) STATCOM has much lower losses than (RSC) [4], iii) because of the large time constant of their field circuit, the control on these machines is not fast enough to compensate when the load changes speedy, iv) short circuit current contributing.

1.3.1 The Importance of (STATCOM) and Its Applications

The corresponding application benefits for STATCOM can be made in terms of its applications and operational characteristics:

1. V-I Characteristics: STATCOM can insert its full reactive current even about 0.2 pu system voltage level at very low one. This makes STATCOM superior to SVC in providing voltage support under large system disturbances. Under large disturbances in the system, STATCOM is excellent to provide voltage upholding. The maximum current of STATCOM is precisely specified by the capacitor and inductor size because it has increased transient rating in both inductive and capacitive region.

2. Transient Stability: STATCOM is very active in enhancing the transient stability of transmission system because of its capability to remain full reactive (capacitive) current at low system voltage

3. Response Time: The existence of fully controllable power semiconductors in STATCOM makes its closed loop bandwidth and accessible response time are significantly better than those of SVC. The fully controllable power semiconductor switches with a switching frequency at supply frequency makes STATCOM supplies significant response and stable operation at large changing in transmission network impedance.

4. Exchange Real Power Ability: STATCOM increases power system efficiency, enhances stability limits, improves dynamic compensation and prohibit

power outages by exchanging and controlling of active and reactive power independently when it links the ac power system with a suitable energy storage (super conducting magnetic storage, battery or large capacitor, etc).

5. Installation and Physical Size: The relatively small size energy storage in the dc-link makes STATCOM converter enhances system replicability, a significant reduction in overall size (reported as 30-40% in [3]), installation action and cost.

1.3.2 The Types of (STATCOM) and Its Varies Properties

The converter which produces controlled reactive power has two types: i) current source type (CSC) that is proposed in this thesis ii) voltage source type (VSC). However, high using of voltage source converter because of the following advantages [3].

1. The bi- directional voltage blocking capability of power semiconductors is the Current source converters requirements. The gate turn-off capacity of the existing high power semiconductors (IGBTs, GTOs) makes them to block reverse voltage with prejudicial effect on the other parameters or cannot do it at all.
2. The losses of dc-link capacitor is practically less than that of dc-link reactor of CSC.
3. VSC involves on capacitors which may be supplied directly because of the leakage inductance of the coupling transformer at its ac terminals while the CSC needs to reactors.

STATCOM systems are described according to their using as i) Distribution STATCOM (DSTATCOM) which works as load compensation i.e. load balancing, power factor correction and filtering of harmonic ii)Transmission STATCOM which controls on the reactive power flow in the transmission system [1,5]. STATCOM is used to inject or absorb required reactive power at faults cases or heavy loading case as it is proposed in this work. Then, reactive power per phase produced by the converter can be expressed as follows [3], The converter of VSC which supplied by dc-link capacitor, C , from a dc side generates output three-phase voltage based controlled on the ac side and has the same frequency of ac power system. The output voltage of the converter for each phase has the same angle with each phase voltage of the ac system and is coupled together by coupling reactor between of them

(excluding the coupling transformer reactance). It will generate the reactive power for each phase and can be mentioned as follows [3].

$$Q = \left(\frac{V - V_0}{X} \right) V = \frac{1 - \left(\frac{V_0}{V} \right)^2}{X} V^2$$

The converter produces reactive (inductive) power when the magnitude of ac system voltage (V) is bigger than that of output voltage for the converter (V₀). Otherwise it will give reactive (capacitive) power when its output voltage magnitude (V₀) is higher than that of ac system voltage (V). In the actual STATCOM implementations, all of the applied converters consist of several number of rudimentary converters. In transmission STATCOM systems, multiphase converter topologies and compound coupling transformer connections eliminate the harmonics that produced by VSC when fully controllable power semiconductors (GTO, GCT) are switched at supply frequency.

1.4 Literature Survey

Although the prospect use of CSCs for reactive power compensation has been recognized more than 35 year [3, 7], the electrical engineers did not realize it for many years. The first application of line commutated rectifiers was the beginning for exploitation of current source converter topology. Line commutated rectifiers included line commutated thyristors without ac capacitors. The capacitors at ac side give low impedance for high order harmonics injected by the converter and commutation path for the currents of power semiconductors because of forced commutated power semiconductors for fundamental topology of CSC.

The advents in power semiconductor and capacitor technology have made PWM voltage source converters popular in power electronics, leaving application of CSC as line commutated thyristorized front end rectifiers in DC drives, or load-commutated thyristorized inverters in MV synchronous motor drives. PWM CSC has organized wide implementation in MV AC drives due to reliable ingrained short circuit protection, motor friendly waveforms and simple converter topology of GTOs and GCT s introduction [8],[9]. MV drives applied CSC with PWM as dc motor drive and an active rectifier for front end instead line commutated thyristor rectifiers, thus removing their ingrained characteristics such as distorted line currents and bad

power factor [10],[13],[14]. A. Weber, E. Carroll and M. Frecker discussed the implementing of single phase CSC as a resonant inverter in induction heating in 2002 [15].

Rectifier or inverter is the basic function of CSC according to the research work. It has control modulation performances and control schemes and modulation performances have been reported consequently [16-17]. However, the researches on CSC based STATCOM is less than that of VSC based STATCOM [7-18].

A reactive power compensation system which employs a three-phase PWM current source converter which is modulated by optimized PWM patterns stored in an EPROM is presented in [7]. L. Moran, P. Ziogas, G. Joos used optimized PWM patterns stored in an EPROM to modulate a three-phase PWM current source converter for reactive power compensation system function in 1989 [7]. This work also involves phase angle control application to close reactive power demand loop and power semiconductor ratings specification, input filter and dc-link reactor design and optimizing the system response by methods of reactive power current control. The research work of CSC based STATCOM on a 120V, 500VA laboratory Depended on the control of phase angle shift with variable modulation index to make the dc-link current constant and control on reactive power by using (SVPWM) PWM space vector in [19].

For static power compensation, proposed three phase current source converter switched by integrating H-type smooth switching module to decrease losses of switching [20]. This topology used control of phase shift angle and trapezoidal PWM with a carrier frequency of 5kHz on low voltage scaled proto type to enhance efficiency at cost of maximum control and circuit complication.

The state space representation of CSC based STATCOM in dq frame is used to Implement integral controllers and full state- feedback to remove oscillations because of poorly damped input filter at CSC response improving and resulted in simultaneous between phase shift angle and modulation index control in [21].

New approach has been depended to linearize state space representation of CSC based STATCOM in [22]. It uses CSC based STATCOM with SVPWM modulation and decoupled state feedback controller to clarify very short response time at a relatively low switching frequency of 900Hz, outstanding voltage and current waveforms.

A comparison between CSC based STATCOM and VSC based STATCOM has been given in [23] according to their start-up and cost, dc-link energy storage requirement, ac-side waveform quality and device rating. This comparison study displays that CSC based STATCOM has certain benefits over VSC based STATCOM in following points: CSC based STATCOM, i) does not inject harmonics in the “idle” state ii) can submit better ac current waveforms at relatively lower switching frequency iii) does not need inflow current limiting or pre-charging scheme. Poor voltage regulation and self-excitation problems have been solved by employing CSC based STATCOM to compensate induction generators in [24]. The parallel-cell multilevel CSC based STATCOM and that with symmetrical Emitter Turn-off Thyristor (ETO) are proposed in [25]. Its control, power stage design, switching modulation and modeling scheme are explained and analyzed by simulations. In summary, few researchers has interested with designing and analyzing CSC based STATCOM systems [18]. However, different PWM techniques and VAR control methods can be increasingly applied with the advents in HV-IGBT and IGCT technologies in the future.

1.5 Significance of The Study

In this research work, it is aimed at developing the simplest CSC based STATCOM topology for power system applications and it depends on [37]. Its circuit diagram has already given in Fig.1.3a. The Continuing problems in the power system is the voltage drop of power system buses when it exposes to different faults or suddenly large loads. The inductive characteristics will increase in this case. CSC-STATCOM will behave as capacitive system and inject the required reactive power to the bus of the power system. The magnitude of reactive power depends on the phase shift angle value between the bus voltage wave and the fundamental components of the AC side line current. This angle can be controlled by switching signals applied to power electronic switches by SPWM technique. The proposed method will utilize pole placement control to vary this shift angle by controlling modulation index components (M_d and M_q) to get better response. The pole placement control depends on calculating K matrix at desired poles positions to make the system stable.

1.6 Organization of the Dissertation

After discussing chapter 1 and its contents, the organization of dissertation in this thesis is as follows:

In Chapter 2, system description and operating principles of CSC based STATCOM is described. After presenting the basic circuit configuration, the principles of reactive power control in CSC are described. Comparing the applicable modulation techniques for CSC have been explained.

In Chapter 3, reactive power control methods for CSC based STATCOM and two cases for modern control method based on State Feedback-Controller are discussed with the proposed pole shifting controller.

In Chapter 4, the simulation of power system circuit with utilizing CSC-STATCOM controlled by pole placement method and the results figures have been discussed under different cases of disturbances applied to the circuit.

Chapter 5, this chapter gives general conclusions. Proposals for further work are also given in the same chapter.

In Appendix A, the derivation of CSC based STATCOM model in dq stationary frame is presented.

In Appendix B, the calculations of K, J and N matrices have been calculated in mat lab with the existence of A, B,C,F as known matrices

CHAPTER TWO

SYSTEM DESCRIPTION AND OPERATING PRINCIPLES OF CURRENT SOURCE CONVERTER BASED STATCOM

2.1 Introduction

CSC based STATCOM is a compensator which is shunt connected to supply three phase balanced currents with adaptable magnitudes and nearly sinusoidal. These currents are lagging or leading line system voltages by nearly 90 to compensate oscillating reactive power in power system at disturbance cases or balanced loads with reactive power oscillating such as asynchronous or synchronous motors in Ward-Leonard drives. The Current Source Converter system will be described with principles of operating in this chapter to attain these following points:

1. STATCOM generates reactive current component quantity should be controlled between specific value and zero.
2. The reactive power injected to the power system explains STATCOM current to be leading or lagging the voltage of ac supply.

Basic circuit study selected for the CSC based STATCOM. After that, its operating principles during reactive power control will be clarified. Its reactive power control will be clarified with operating basics. CSC creates closely sinusoidal currents by applying different modulation techniques will be explained here.

2.2 Basic Circuit Arrangement

Current Source Converter (CSC) for three phase type works with six fully controllable power semiconductor switches (S1, S2, S3, S4, S5, S6) which include bipolar voltage blocking capabilities and unidirectional current carrying as displayed in Fig 2.1 [19].

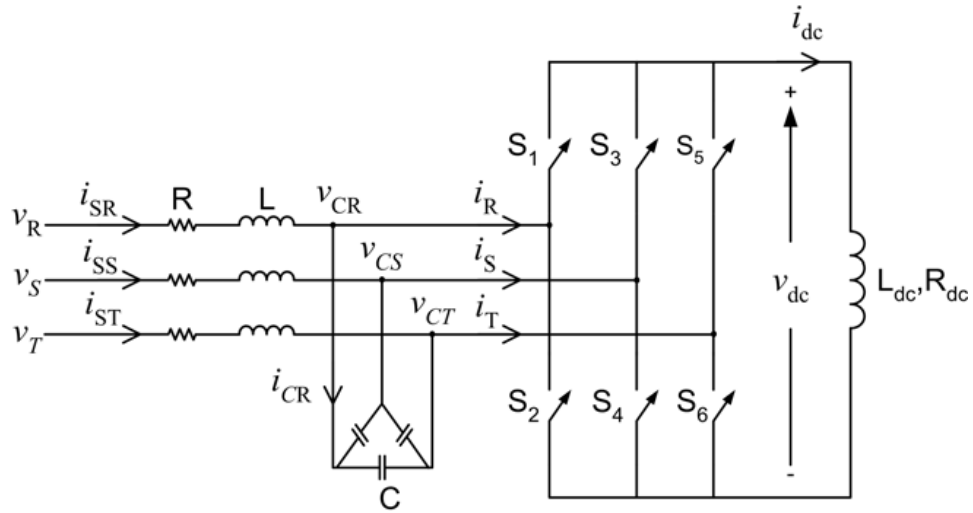


Figure 2.1: Topology of three phase current source converter for general circuit.

A dc-link reactor has been placed in dc-link as the energy storage element is dc-link reactor with dc-link inductance L_{dc} and resistance R_{dc} are connected in series at dc side as equivalent circuit. The current (I_{dc}) is closely constant along a switching period because the time constant of dc-side circuit is very high.

The converter line currents (i.e., i_R , i_S , and i_T in Fig.2.1) include harmonics with the fundamental component at supply frequency in the form of current pulses in two directions due to the power semiconductors switching at the steady state. By connecting three phase low-pass filter at the AC side of the converter, almost sinusoidal supply line currents (i.e., i_{SR} , i_{SS} , i_{ST}) can be obtained with filtering out these harmonics [26]. The converter current pulses can be provided with a low impedance return path by complying CSC to capacitors in the input filter. The harmonic content of the injected currents effectively decreases with regulating the nook frequency by the use of series reactors in the input filter. The external reactor inductance, cable, coupling transformer leakage inductance and bulbar inductances form the filter inductance. an external reactor in each line have been used to fine set the corner frequency on AC side as shown in Fig.2.1. The series resistance, R takes account of internal resistances of external filter reactor, cables, coupling transformer and bus bars to provide electrical damping In the input filter.

2.3 Principles of Reactive Power Control

The relation between input and output sides in CSC to control the generating of reactive power will be described in steady-state with canceling the filter at AC side as shown in Fig. 2.2.

Following assumptions are made in the derivations:

- 1) Ignoring the losses of power semiconductor switches.
- 2) the dc-link current (I_{dc}) is approximately constant with ignoring small ripple because of the high time constant (L_{dc}/R_{dc}) during switching period.
- 3) three phase purely sinusoidal AC supply voltages are balanced as in (2.1).

$$\left. \begin{aligned} v_R &= V \cos(\omega t) \\ v_S &= V \cos(\omega t - 2\pi/3) \\ v_T &= V \cos(\omega t - 4\pi/3) \end{aligned} \right\} \quad (2.1)$$

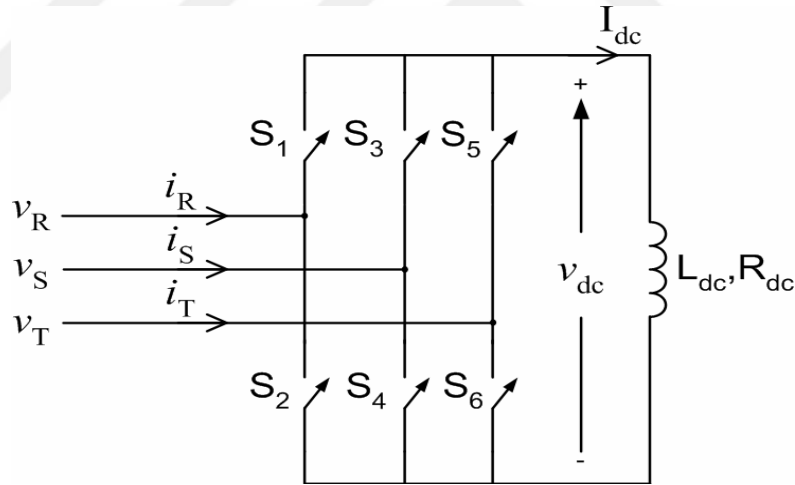


Figure 2.2: CSC Circuit diagram without input filter.

There are typical switching signal for each power semiconductor switches injected by applying modulation techniques (m_{S1} , m_{S2} , m_{S3} , m_{S4} , m_{S5} , m_{S6}). The converter line current and switching signals for the first leg i_R , m_{S1} , m_{S2} are shown in Fig.2.3.

The switching signals and the corresponding converter line currents are the same in shape in all three lines but they are shifted by there are shift angles by $2\pi/3$

and $4\pi/3$ radians for converter line currents (i_s , i_T) and switching signals (m_{S3} , m_{S4} , m_{S5} , m_{S6}) than those of line R.

The Instantaneous expression of line currents values can be described as in (2.2) [27].

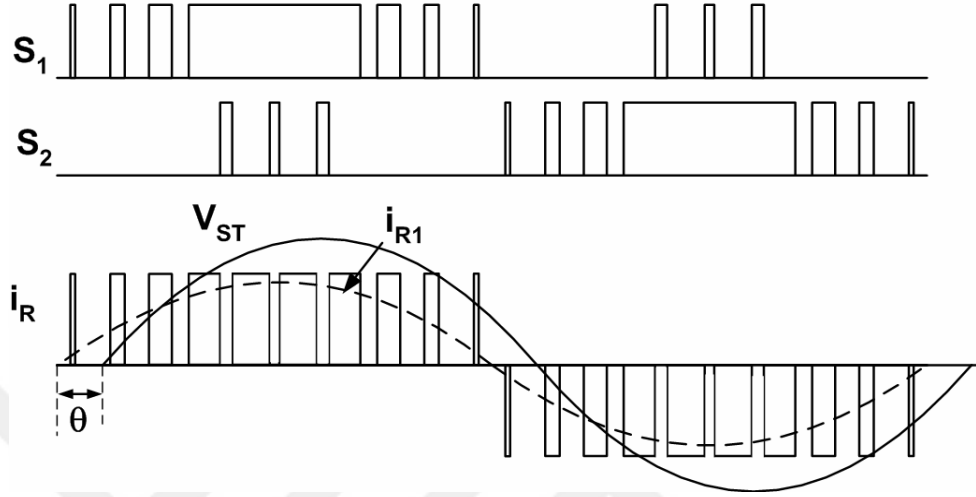


Figure 2.3: Switching signals of S1&S2, and the corresponding theoretical converter input current, $i_R(t)$ and line-to-line voltage, $v_{ST}(t)$ for inductive reactive power.

$$\left. \begin{aligned} i_R(t) &= (m_{S1} - m_{S2})I_{dc} \\ i_S(t) &= (m_{S3} - m_{S4})I_{dc} \\ i_T(t) &= (m_{S5} - m_{S6})I_{dc} \end{aligned} \right\} \quad (2.2)$$

The Converter line currents can be written in Fourier series extension as in (2.3).

$$\left. \begin{aligned} i_R &= I_1 \sin(\omega t + \theta) + \sum_{h=2}^{\infty} I_h \sin(\omega_h t - \lambda_h) \\ i_S &= I_1 \sin(\omega t + \theta - 2\pi/3) + \sum_{h=2}^{\infty} I_h \sin(\omega_h t - \xi_h) \\ i_T &= I_1 \sin(\omega t + \theta - 4\pi/3) + \sum_{h=2}^{\infty} I_h \sin(\omega_h t - \Psi_h) \end{aligned} \right\} \quad (2.3)$$

Modulation index, M is realized as in (2.4) [28,13].

$$M = \frac{I_1}{I_{dc}} \quad (2.4)$$

Harmonic components in (2.3) can be ignored with staying the fundamental component of preponderant harmonic current that generated by CSC. This mean that the power system deals with reactive and active power of CSC at the same frequency of the power system.

By depending on (2.2), (2.3) and (2.4), fundamental line currents of CSC can be written in dc-link current, I_{dc} and modulation index, M terms as in (2.5).

$$\left. \begin{aligned} i_{R1} &= MI_{dc} \sin(\omega t + \theta) \\ i_{S1} &= MI_{dc} \sin(\omega t + \theta - 2\pi/3) \\ i_{T1} &= MI_{dc} \sin(\omega t + \theta - 4\pi/3) \end{aligned} \right\} \quad (2.5)$$

The specified values in (2.1) and (2.5) can be explained by phasor diagrams as in Fig. 2.4. When CSC creates capacitive reactive power, its ac line currents leads system line-to-line voltages by (θ) radians or lags system line voltages by $(\pi/2 - \theta)$ radians if it takes inductive reactive power as shown also in Fig. 2.3. The difference between capacitive and inductive modes that the switching signals in capacitive mode must be displaced by closely π radians than that of inductive mode to lead line currents by an angle θ as in Fig. 2.4b and Fig. 2.5.

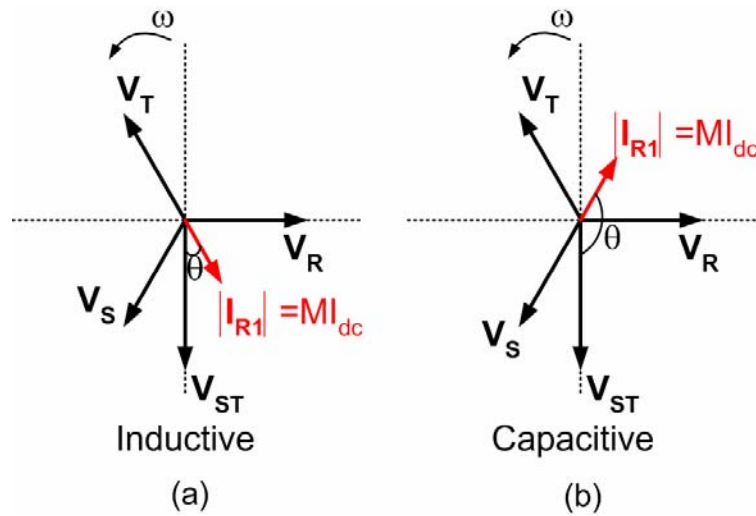


Figure 2.4: Principle phasor diagram of CSC in a steady-state (a) for inductive (b) capacitive reactive power generation.

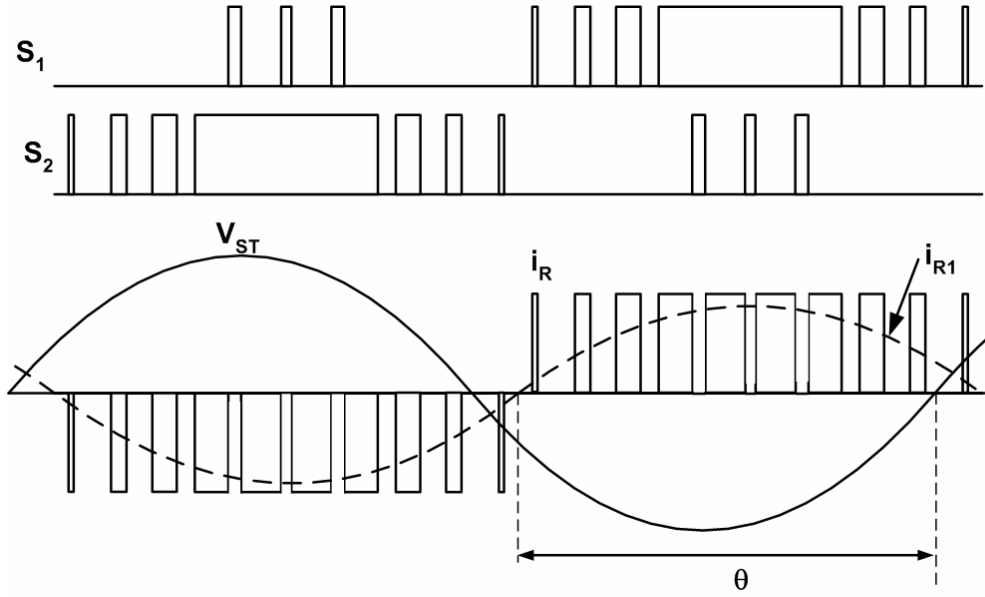


Figure 2.5: Switching signals of S1&S2, and the corresponding theoretical converter input current, $i_R(t)$ and line-to-line voltage, $v_{ST}(t)$ for capacitive reactive power generation of CSC.

Active and reactive steady-state expressions at ac side of CSC can be written as in (2.6) and (2.7) by depending on (2.1), (2.5) and Fig.2.4.

$$P = \frac{3}{2} V M I_{dc} \sin \theta \quad (2.6)$$

$$Q = \frac{3}{2} V M I_{dc} \cos \theta \quad (2.7)$$

The losses in the dc-link side of CSC due to reactor internal resistance, R_{dc} as in (2.8) equal to active power at AC side after neglecting the losses of power semiconductor switches. By compensating (2.6) in (2.8), dc-link voltage and current (V_{dc} , I_{dc}) at steady-state can be written as in (2.9) and (2.10).

$$P = V_{dc} I_{dc} = R_{dc} I_{dc}^2 \quad (2.8)$$

$$V_{dc} = \frac{3}{2} V M \sin \theta \quad (2.9)$$

$$I_{dc} = \frac{3 V M \sin \theta}{2 R_{dc}} \quad (2.10)$$

Active and reactive power components can be substituted by (2.11) and (2.12) respectively by using (2.10) in (2.6) and (2.7). When active power cannot be delivered by CSC at steady-state, the range of θ for the expressions in (2.11) and (2.12) is only $[0, \pi]$ because active component becomes negative after (π) .

$$P = \frac{9 V^2 M^2}{4 R_{dc}} \sin^2 \theta \quad (2.11)$$

$$Q = \frac{9 V^2 M^2}{8 R_{dc}} \sin 2\theta \quad (2.12)$$

Where $0 \leq \theta \leq \pi$

Active power and reactive power increases both of them at the range $[0, \pi/4]$ of phase angle θ by depending on (2.11) and (2.12) as given in Fig.2.6. The same conception can be completed for the area between $3\pi/4$ and π of θ . These operating ranges are marked by shaded areas in Fig.2.6. CSC behaves as controller for active power flow for θ between $\pi/4$ to $3\pi/4$ and delivers active power from ac system. It can be noted from Fig.2.6 that the maximum reactive power at $\pi/4$ is smaller than maximum active power at $\pi/2$ by half time. This allows to connect on two networks with different frequencies together by CSC back-to-back circuits and control on both reactive and active power flow between these networks. The requirement of active power flow just for recovering STATCOM power losses and remaining dc-link active makes the need of reactive power control is much higher than active power flow in steady-state. The energy stored content of dc-link reactor can be changed by extracting large values of active power in transient state with a short time period for the operation of CSC in STATCOM mode.

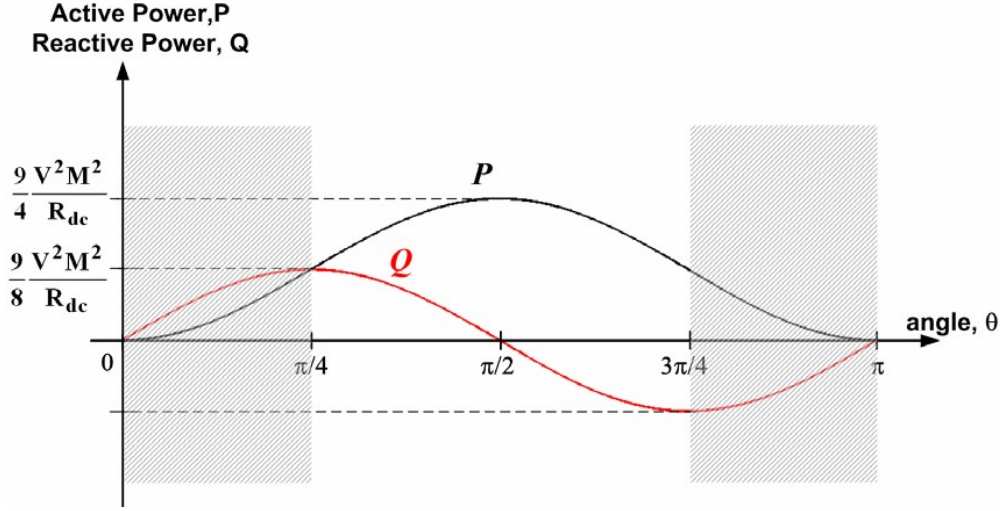


Figure 2.6: Theoretical active and reactive power variations of CSC STATCOM w.r.t. angle, θ at a fixed modulation index.

The expressions of (2.13) and (2.14) can be considered as alternatives of that in (2.6) and (2.7) for active and reactive power because of closing θ to 0 in the inductive region and to π in the capacitive region for the operation of STATCOM in steady-state.

$$P = \frac{3}{2} V M I_{dc} \phi \quad \text{where } \phi = \begin{cases} \theta & \text{for inductive region} \\ \pi - \theta & \text{for capacitive region} \end{cases} \quad (2.13)$$

$$Q = \begin{cases} \frac{3}{2} V M I_{dc} & \text{for inductive region} \\ -\frac{3}{2} V M I_{dc} & \text{for capacitive region} \end{cases} \quad (2.14)$$

The control methods of reactive power generated by CSC control by depending on (2.14) are i) dc-link control, I_{dc} , ii) modulation index, M , or iii) both of them. The pulse widths change for all pulses at specific factor in case of modulation index modifying. The changing of phase shift angle ϕ in (2.13) causes increasing or decreasing dc-link current value when delivers or extracts active power as seen by equating (2.13) to (2.8) to result in (2.15).

$$I_{dc} = \frac{3 V M}{2 R_{dc}} \phi \quad \text{where } \phi = \begin{cases} \theta & \text{for inductive region} \\ \pi - \theta & \text{for capacitive region} \end{cases} \quad (2.15)$$

The energy storage element makes dc-link voltage in VSC and dc-link current in CSC approximately constant without any active power dissipation and its inductance does not effect on the reactive power. Therefore, “Static VAR Compensator with minimum energy storage element” is called on the STATCOM.

Fixing phase shift angle ϕ at zero in (2.13) and considering $R_{dc}=0$ with ideally all power semiconductors (lossless CSC) prevent flowing of active power to CSC in steady-state. The zero values of ϕ and R_{dc} do not define the equation (2.15). Providing a power flow from/to CSC by varying ϕ to control dc-link current magnitude and this causes the dc-link reactor to charge and discharge to specific dc-link current value as seen in Fig 2.7. The charging area of dc-link reactor is located at quadrants (I, IV) and the discharging area is located at (II, III) quadrants for current phasors as in Fig.2.7. Then, Modulation index technique controls on regulating the required reactive power as in Fig.2.8.

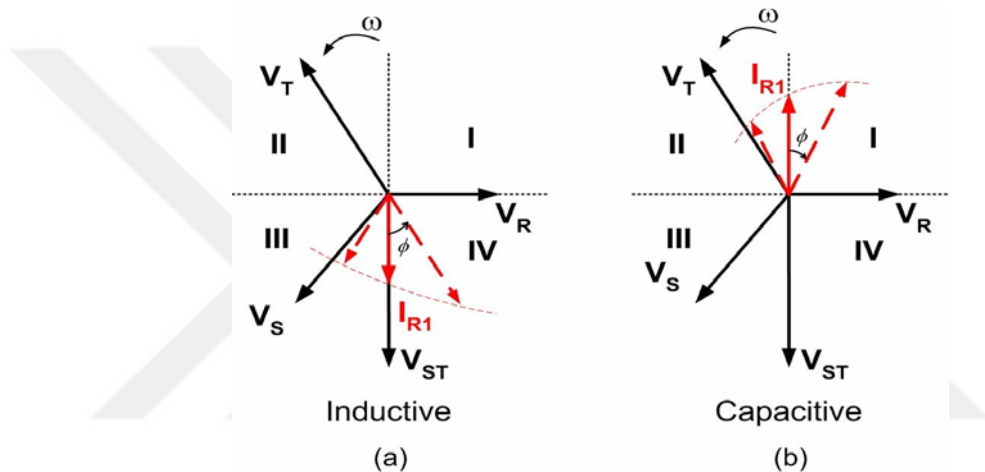


Figure 2.7: Phasor diagram of CSC in a lossless system (transient-state representation) for inductive (a) capacitive reactive power generation.

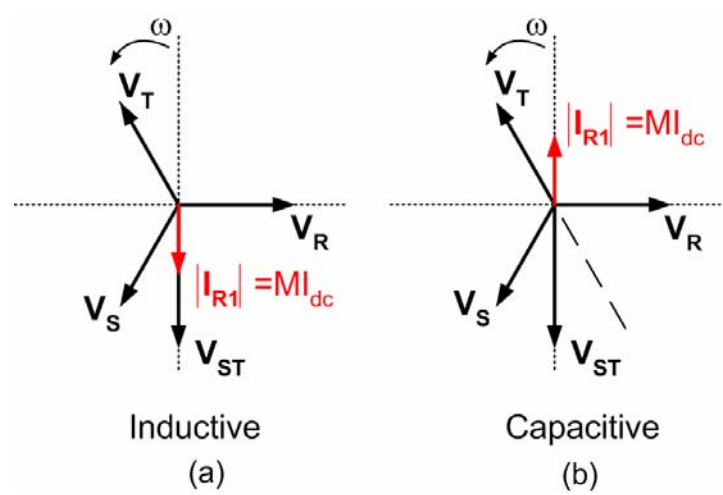


Figure 2.8: Phasor diagram of CSC in a lossless system (steady-state representation) (a)for inductive (b)capacitive reactive power generation.

Reactive power generation of CSC can be achieved by Synchronizing phase shift angle control with modulation index, M to get a quicker response as shown in [21-22]. However, in some applications, modulation index control is inappropriate, as to be shown in Section 2.3. Therefore, phase angle via dc-link current control is used to regulate reactive power and charge and discharge dc-link reactor. The simulations and laboratory experiments explained fact that M and ϕ simultaneous control is faster than the control of ϕ only in response case as given in [21].

CSC needs to input filter at AC side in a practical system which is neglected in Fig.2.2 to filter out the harmonics of line current that shown in Fig.2.3 and Fig.2.5. The input filter works as voltage regulator at the CSC input terminals. Fig.2.9 shows If The supply or system voltage is constant V_R , CSC behaves as capacitive mode when its input voltage V_{CR} becomes bigger than V_R and decreasing V_{CR} under V_R leads CSC to work in inductive mode and absorb reactive power. The filter inductances values play a role in transporting V_{CR} from full capacitive load to full inductive load as shown in Fig.2.9 and Fig.2.10 for single line diagram of CSC and both of its operation modes as Phasor diagrams respectively.

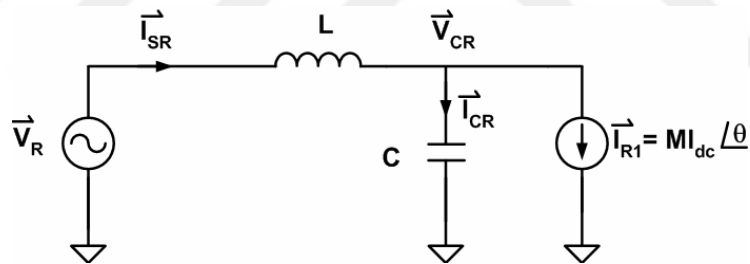


Figure 2.9: Equivalent single line diagram of CSC based STATCOM.

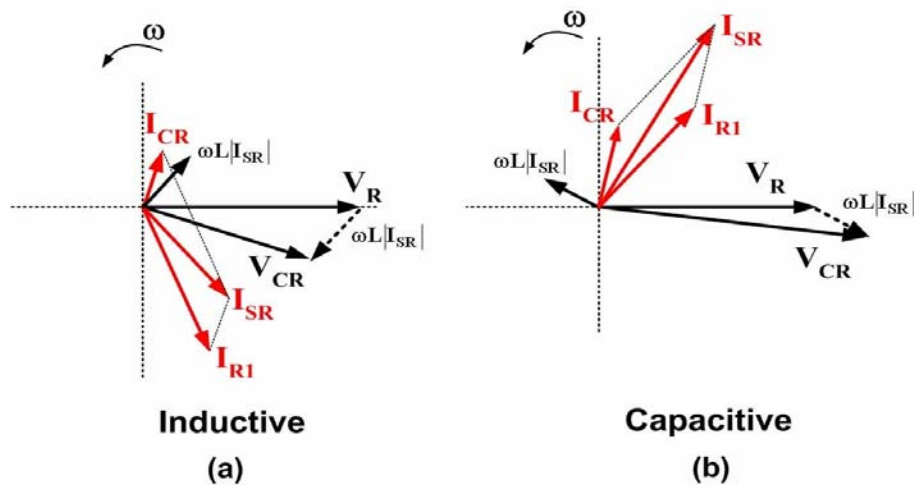


Figure 2.10: Illustration of variations in converter input voltage, V_{CR} with the generated reactive power of CSC.

2.4 Pulse Width Modulation Techniques

Several pulse width modulation techniques have been applied to power converters with the expansion in high speed digital processors and fully controllable power semiconductors [10]. PWM techniques present i) superior control characteristics ii) nearly sinusoidal input/output waveforms, iii) efficient, more compact systems and cost effective [28].

The dc-link current needs to circulating path over the converter or supply and this happens by making one switch from the lower half bridge (S2, S4, S6) at least conducts with at least one switch from the upper half bridge (S1, S3, S5). It can be achieved by Guaranteeing the qualification in (2.16) for the application of PWM techniques to CSC that shown in Fig.2.1.

$$\begin{aligned}m_{s1} + m_{s3} + m_{s5} &= 1 \\m_{s2} + m_{s4} + m_{s6} &= 1\end{aligned}\tag{2.16}$$

CSC has been Exploited with several studies for PWM techniques [30]. The main techniques that used of these studies are i) Space Vector PWM (SVPWM) [35],: ii) Modified Sinusoidal PWM (MSPWM) [10], iii) Selective Harmonic Elimination Method (SHEM) [30].

The three different pulse width modulation techniques have been explained in Fig.2.11, Fig. 2.12 and Fig 2.13 for the corresponding converter line currents and switching styles that mentioned in (2.2). These techniques donate harmonic concatenation of converter line currents as given in Fig. 2.14 that shown as (I_{dc}) via normalized form. Converter line current has theoretically dc-link current value (I_{dc}) as pulses peak value.

Table 2.1. appears the difference between these modulation techniques. CSC operates today on modified version of MSPWM instead of the classical SPWM.

When the converter semiconductors are switched on and off, MSPWM results in lower low order harmonics (such as 5th, 7th, 11th, 13th) at high frequencies like 2kHz if it compared with SVPWM. The modulation technique highly used Today is SVPWM.

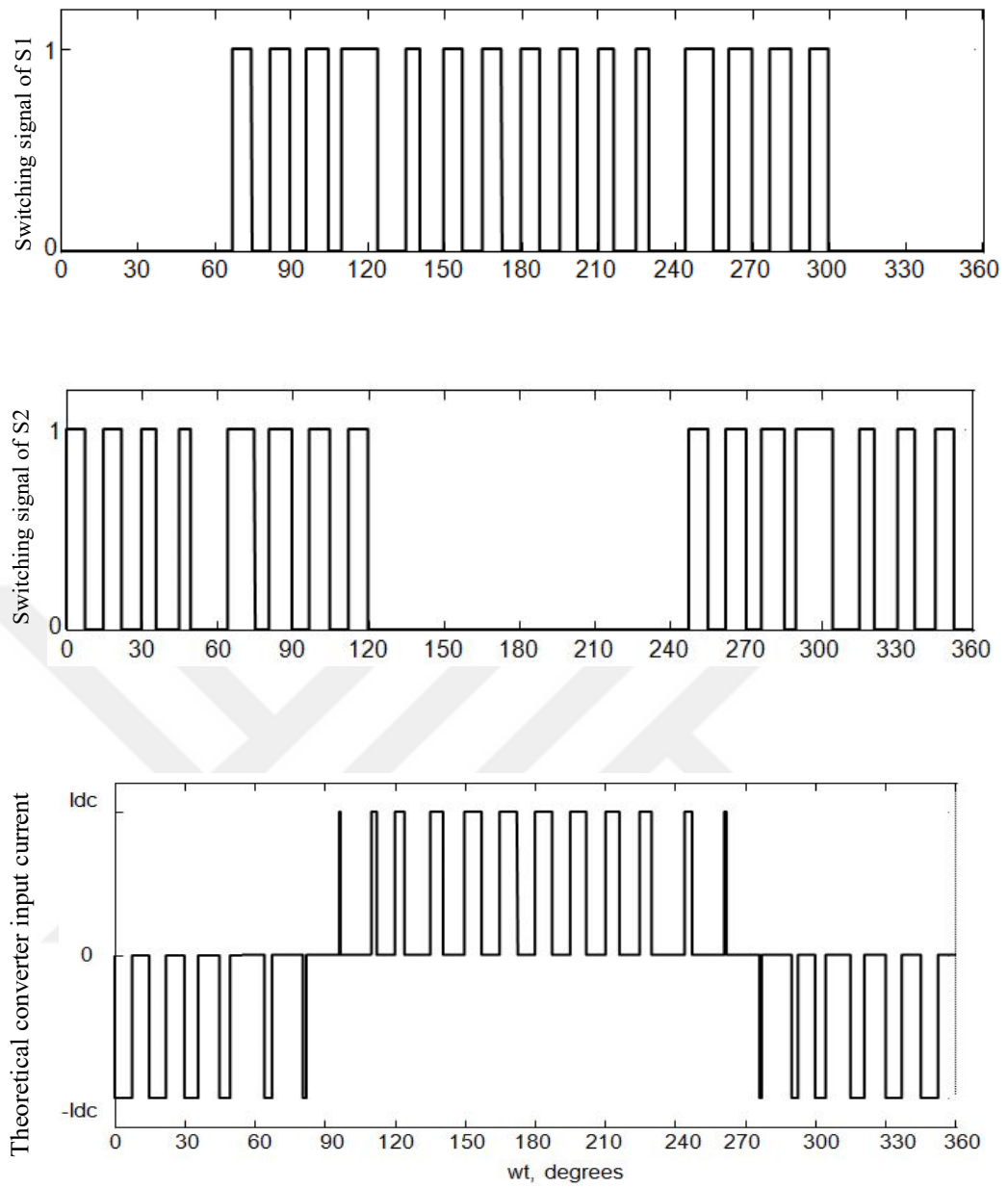


Figure 2.11: Typical switching patterns for MSPWM ($M=0.5, f_{carrier}= 1200\text{Hz}$).

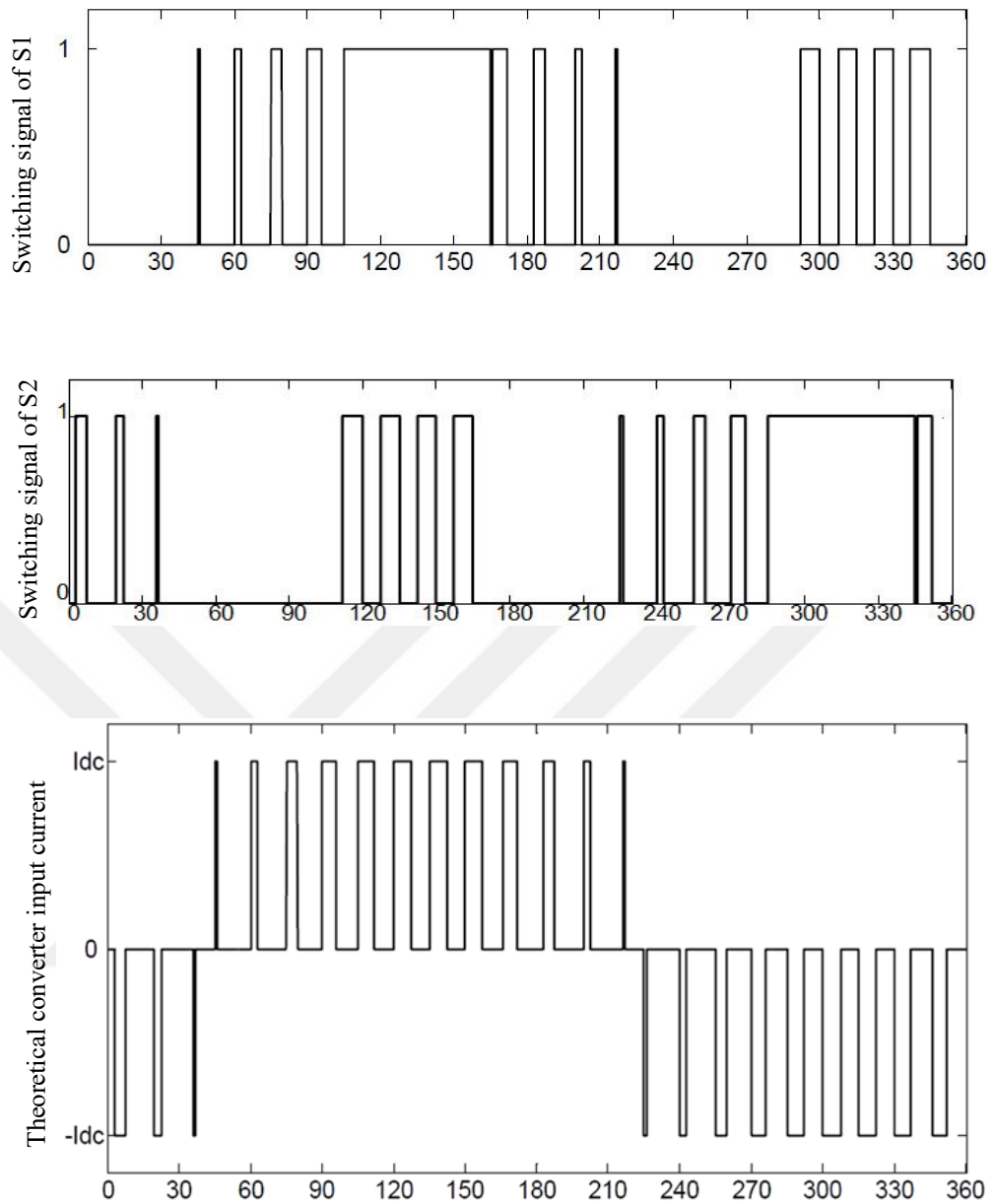


Figure 2.12: Typical switching patterns for SVPWM ($M=0.5$, $f_{carrier}=1200\text{Hz}$).

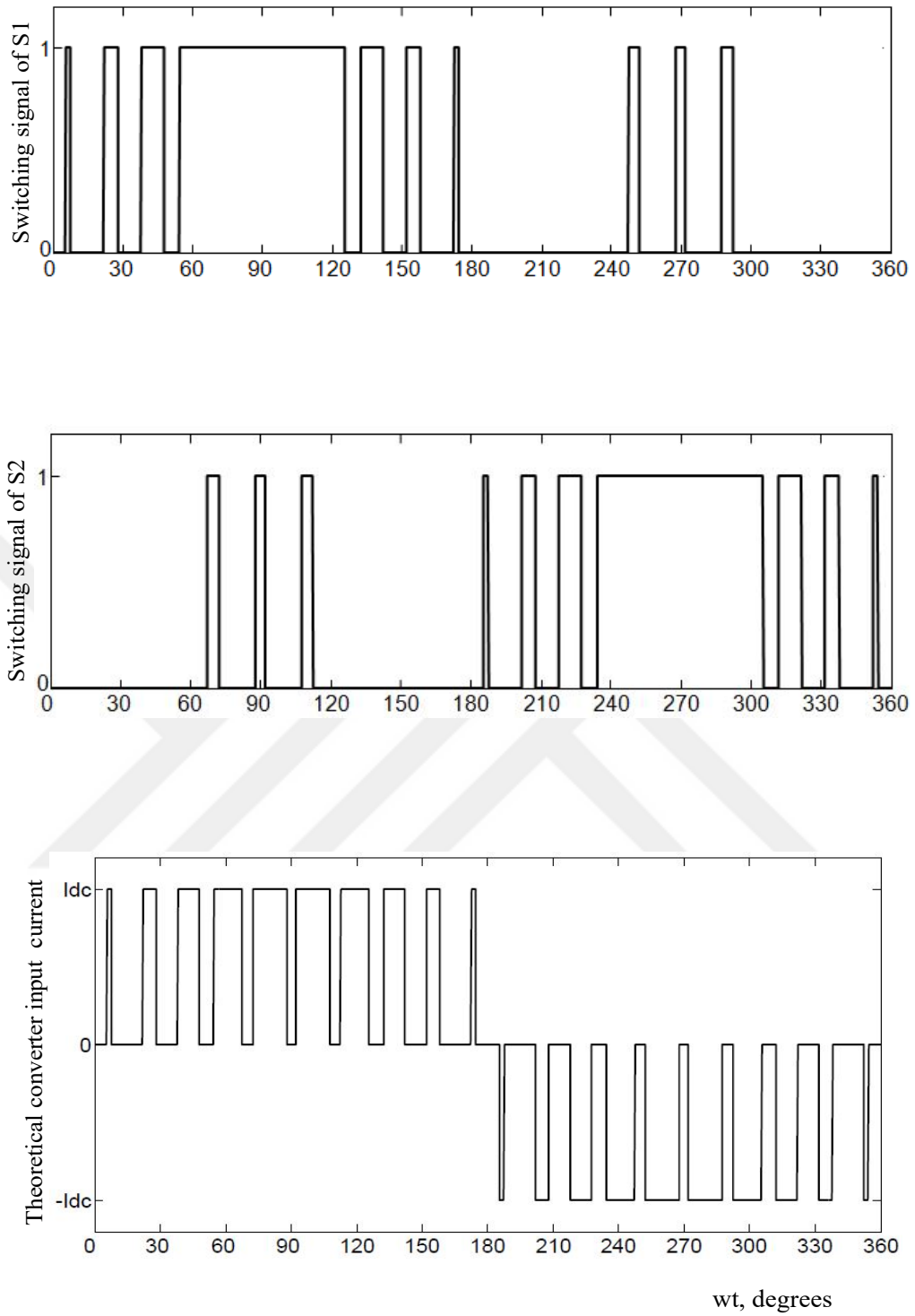
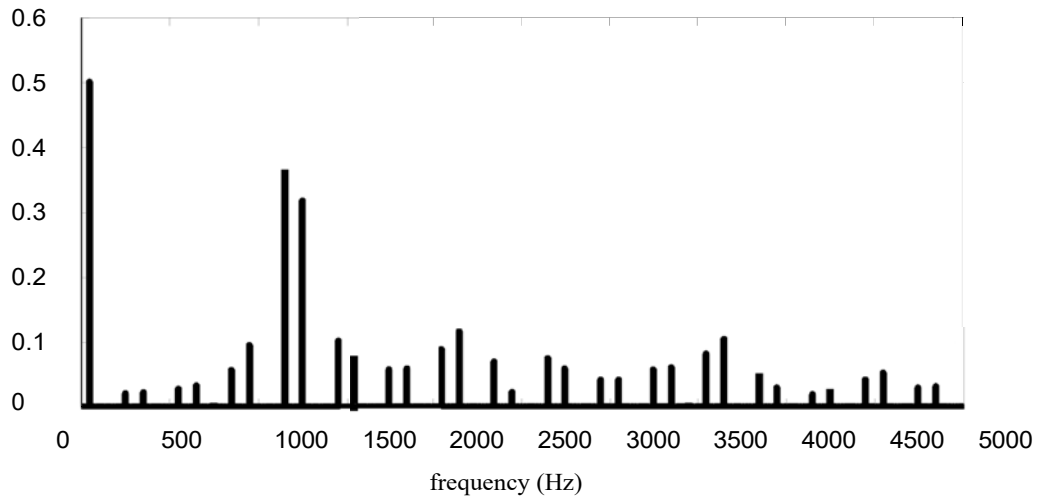
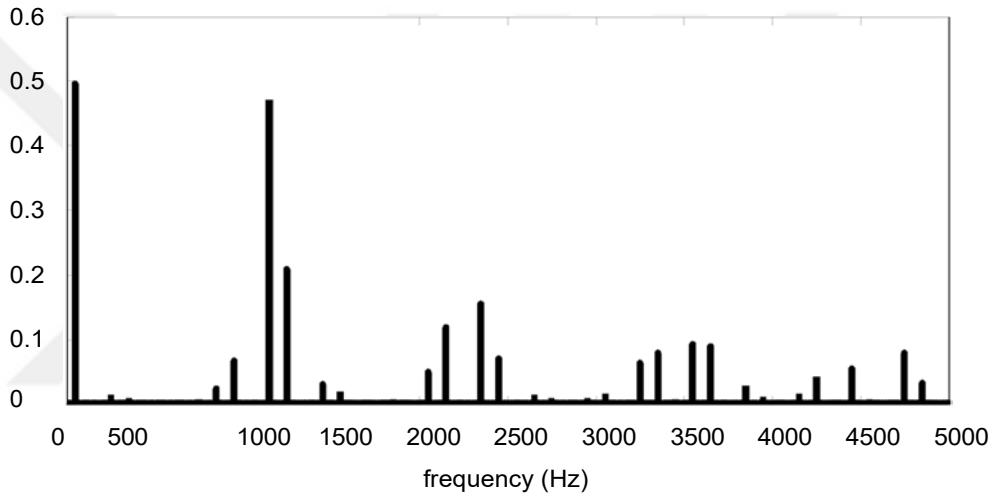


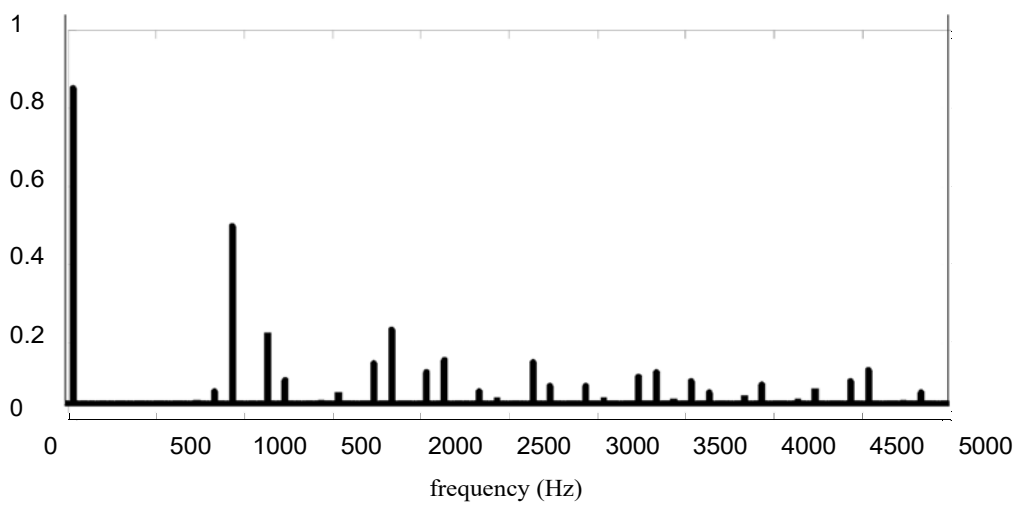
Figure 2.13: Typical switching patterns for SHEM (elimination of 5th, 7th, 11th and 13th harmonics at $M=0.8$).



(a)



(b)



(c)

Figure 2.14: Normalized harmonic spectra of converter input current w.r.t. dc-link current (a) for MSPWM (b) for SVPWM (c) for SHEM.

SVPWM technique for the same carrier frequency has lower switching frequency that makes it widely used today. power applications for low voltage medium use MSPWM because it has control range of modulation index similar to that of SVPWM [10].The simultaneous continuous control of phase shift angle and modulation index for MSPWM and SVPWM cause fast response But, the harmonic spectra of converter line current that produced by SHEM is more than those of SVPWM and MSPWM at low switching frequencies. Using active damping [32, 17] and passive damping [10] avoid the parallel resonance of the input filter in CSC [17] that excited by these low order harmonics. The input filter contains an external damping resistor causes immoderate power dissipation in the Passive damping. On the other hand, active damping requires complicated control algorithm and cannot provide continuous damping in the entire operating range [17].

Table 2.1: Comparison of modulation techniques applicable to CSC.

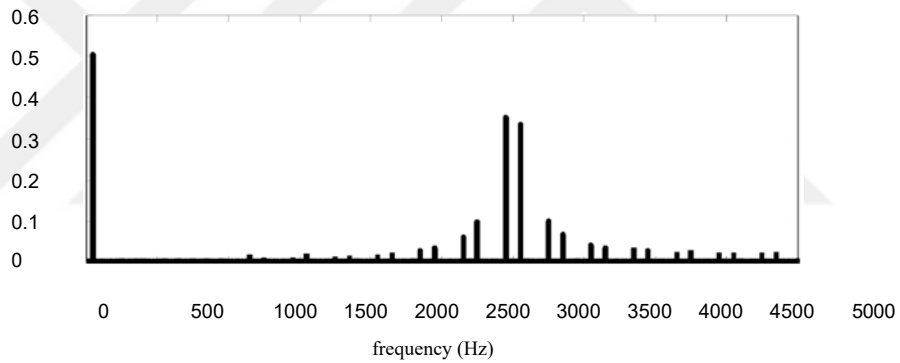
f_s –switching frequency
 f_{carrier} –carrier frequency

K – number of harmonics to be eliminated
 f_1 – fundamental frequency

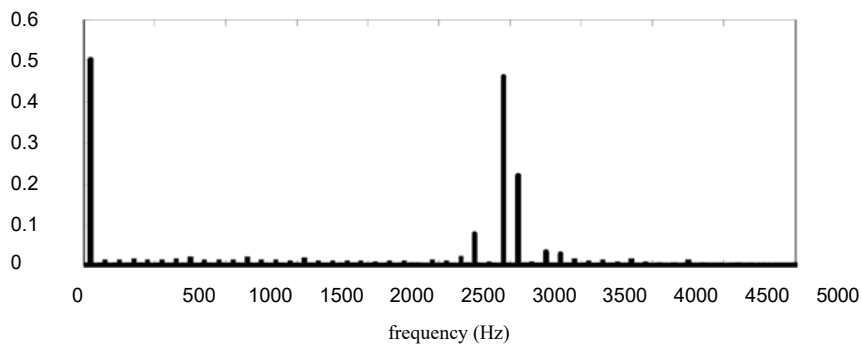
	Harmonic Spectra	Modulation Index	Applications
MSPWM	smaller low order harmonics for $f_s > 2\text{kHz}$ $f_s = (2/3)f_{\text{carrier}}$	controllable $- 0 \leq M \leq 1.0$	medium power IGBT or MOSFET based converters, where $f_s > 2\text{kHz}$
SVPWM	smaller low order harmonics for $f_s < 2\text{kHz}$ $f_s = (1/2)f_{\text{carrier}}$	controllable $- 0 \leq M \leq 1.0$	medium power IGBT or MOSFET based converters, where $f_s > 2\text{kHz}$
SHEM	negligible low order harmonics $f_s = \begin{cases} (2K + 2)f_1 & \text{if } \frac{K}{2} \text{ is even} \\ (2K + 3)f_1 & \text{if } \frac{K}{2} \text{ is odd} \end{cases}$	can only be controlled in discrete steps	Medium or high power IGBT or IGCT based converters where $f_s < 1\text{kHz}$

All modulation techniques used in CSC applications yield the same employment factor for power semiconductors. The average value of the current through each power semiconductor is found to be one third of the dc-link current for all values of modulation index.

SHEM technique is based on pre-calculated switching patterns (i.e., off-line generated pattern) while MSPWM and SVPWM are based on on-line generated patterns [17]. Therefore, patterns of SHEM for each modulation index are to be calculated in such a way that the magnitudes of low order harmonics should be zero as shown in Fig.2.14c. Although the transient response of CSC STATCOM is slower in SHEM, it has been widely used in high power applications, for which switching frequency should be kept at low values, e.g., below 1kHz [18]. In the applications where the switching frequencies above 2kHz is permissible, the use of on-line generated PWM techniques become more feasible, as illustrated in Fig.2.15.



(a)



(b)

Figure 2.15: Normalized harmonic spectra of converter input current w.r.t. dc-link current (a) for MSPWM (b) for SVPWM when carrier frequency, $f_{\text{carrier}}=3\text{kHz}$.

CHAPTER THREE

REACTIVE POWER CONTROL METHOD FOR CURRENT SOURCE CONVERTER BASED STATCOM

The reactive power generated by CSC based STATCOM can be controlled by different control methods which can be classified as: i) PI-type linear controllers for traditional control methods[18], ii) state-space approach for modern control methods[22] and pole placement controller by utilizing state-space representation.

When the fast transient response of the traditional control methods can be achieved by using large proportional gains, the CSC based STATCOM will have large frequency oscillations with the indisposed damped input filter [21]. Therefore, the traditional control methods do not result in an optimal control system with simplicity of their design and implementation [33].

On the other hand, the transient response can be improved by implementing state-space methods that modern control methods depend them because of their chosen closed loop poles. The following benefits of these methods which is designed and implemented by dq-stationary reference frame structure for CSC based STATCOM are i) input filter of CSC will give ingrained damping ii) The control of reactive and active power control will be independent iii) transient response will be faster [34].The following subsections will explain these control methods briefly

3.1 Conventional Control Method based on PI Controller

Phase shift angle (ϕ) and the modulation index (M) are control variables in CSC based STATCOM as explained in Section 2.3. In this method, phase shift angle controls dc-link current value to stay it at reference value $I_{dc}(\text{ref})$. The maximum VAR rating of CSC STATCOM that specify maximum controllable value of modulation index must meet the dc-link current $I_{dc}(\text{ref})$. Fig.3.1 explains The block

diagram of control system for this method. Then, The changing in reactive power is controlled by faster response for this control approach which control the modulation index to generate the required reactive power. The dc-link current control depends on the application type because that staying its magnitude at maximum value for all time causes dc reactor losses and high and high converter losses. The switching signal generator will be provided by phase shift angle and modulation index as inputs to utilize one of modulation techniques as described in Section 2.4.

Another cases utilize the control of dc-link current magnitude through phase shift angle to produce the required reactive power with keeping modulation index fixed without control as shown in Fig.3.2.

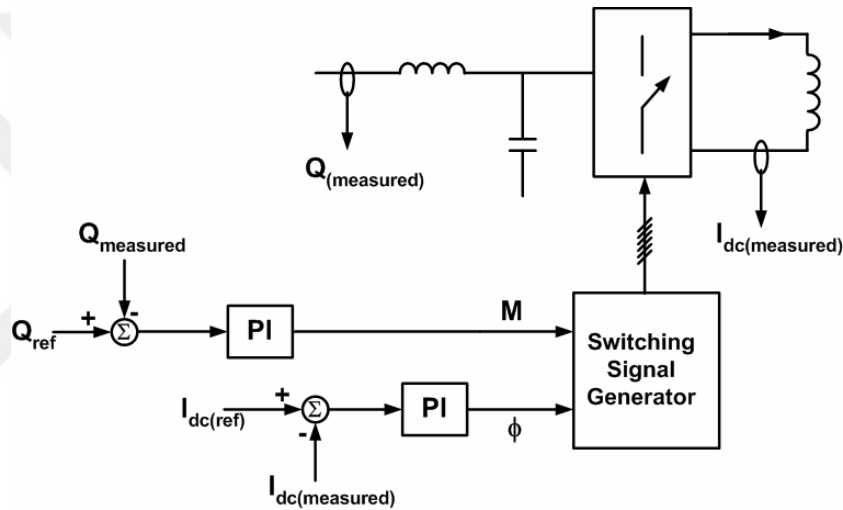


Figure 3.1: Control system based conventional PI controller.

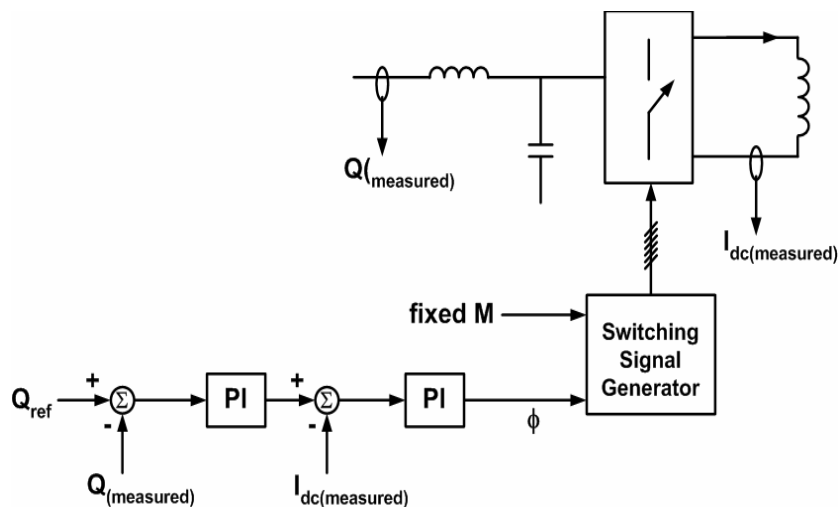


Figure 3.2: Control system based conventional PI controller for CSC based STATCOM, where modulation index control is not applicable.

The Bode diagrams and root-locus plots are graphical techniques which are used together with transfer function to select or design PI parameters for optimum response in the given control system. The system with single input and single output which is called linear time stable systems just can apply these design techniques [33]. These techniques cannot be used for CSC based STATCOM because of its nonlinear characteristics and its multi inputs and multi outputs. Therefore, the Second Method of Ziegler-Nichols Rules which is one of PID tuning rules can be employed to calculate PI parameters for this control system [33]. The control system in Fig.3.2 can also apply this method in steps as in Fig.3.3. Firstly, employing a unit step input to calculate optimum PI parameters of dc-link current controller as shown in Fig.3.3a. Then, applying a step input to the overall control system in Fig.3.3b to utilize pre-determined parameters of dc-link current controller for calculating Best parameters of reactive power controller.

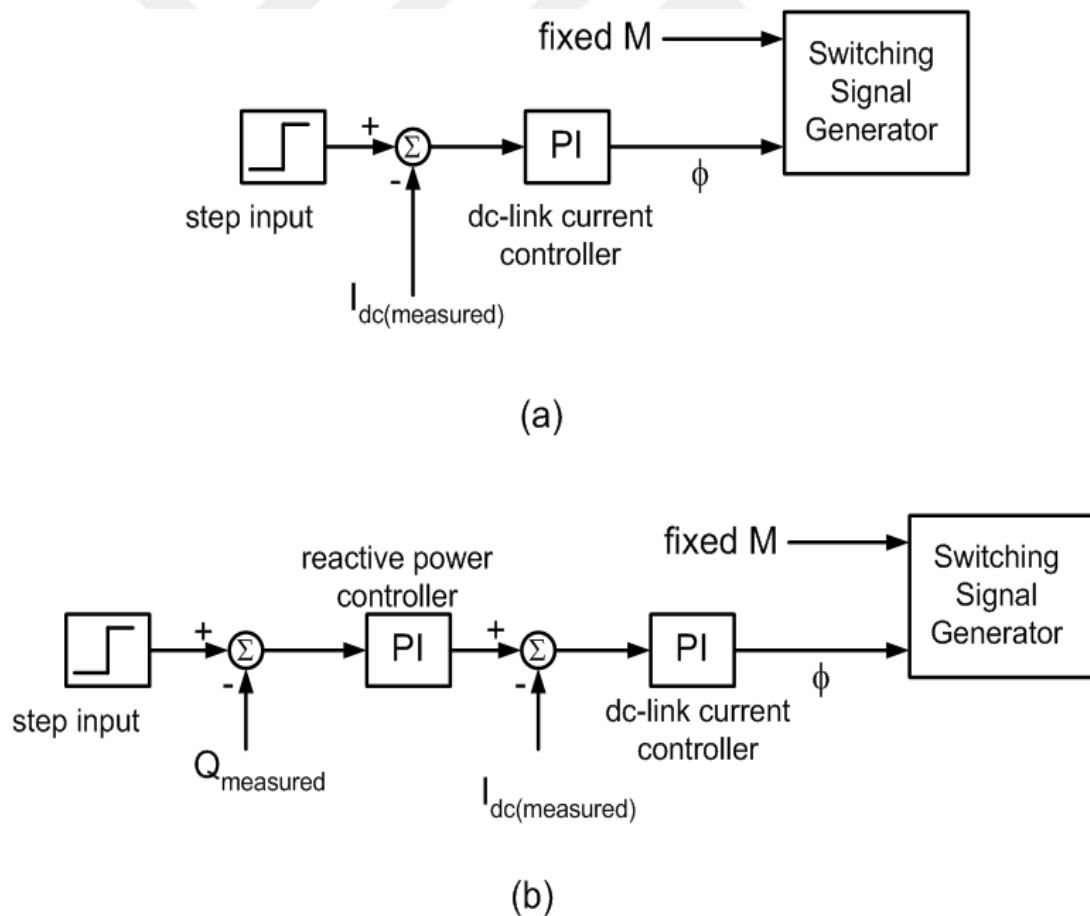


Figure 3.3: Steps applied in tuning PI parameters of CSC based STATCOM control system (a) for dc-link current controller, and (b) for reactive power controller.

3.2 Modern Control Method based on State Feedback-Controller and pole placement controller

To decrease the number of state variables and make them dc amounts in steady-state, d-q stationary frame [34,21-22] must be used to obtain on the state-space representation of CSC based STATCOM for this control method. Fig.3.4 appears the equivalent circuit of CSC based STATCOM and its state-space representation is explained in (3.1) to make both design and analysis of control system comparatively easier. Appendix A explains the derivation of state-space representation. The state-space representation in (3.1) will deduce The equivalent circuit of CSC based STATCOM in Fig.3.5.

$$\frac{d}{dt} \begin{bmatrix} i_{sd} \\ i_{sq} \\ v_{cd} \\ v_{cq} \\ i_{dc} \end{bmatrix} = \begin{bmatrix} -\frac{R}{L} & \omega & -\frac{1}{L} & 0 & 0 \\ -\omega & -\frac{R}{L} & 0 & -\frac{1}{L} & 0 \\ \frac{1}{3C} & 0 & 0 & \omega & -\sqrt{\frac{3M}{23C}} \sin \theta \\ 0 & \frac{1}{3C} & -\omega & 0 & \sqrt{\frac{3M}{23C}} \cos \theta \\ 0 & 0 & \sqrt{\frac{3M}{2Ldc}} \sin \theta & -\sqrt{\frac{3M}{2Ldc}} \cos \theta & -\frac{R_{dc}}{L_{dc}} \end{bmatrix} \begin{bmatrix} i_{sd} \\ i_{sq} \\ v_{cd} \\ v_{cq} \\ i_{dc} \end{bmatrix} + \begin{bmatrix} \frac{1}{L} & 0 \\ 0 & \frac{1}{L} \\ 0 & 0 \\ 0 & 0 \\ 0 & 0 \end{bmatrix} \begin{bmatrix} v_d \\ v_q \end{bmatrix} \quad (3.1)$$

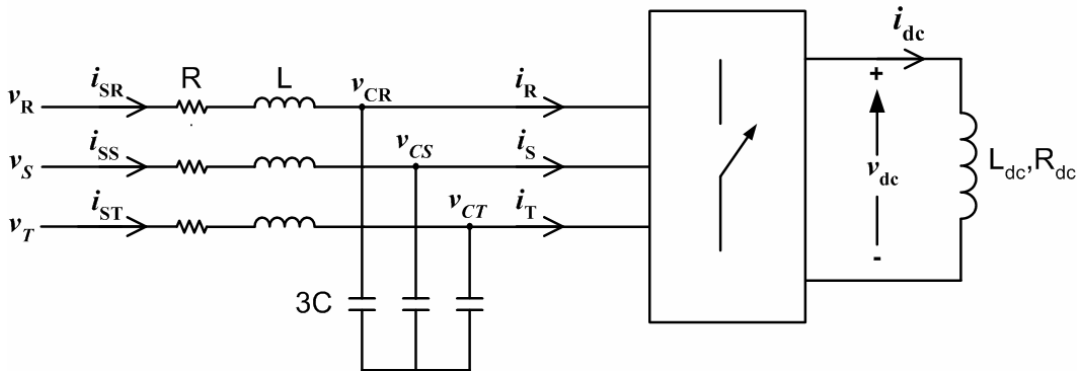
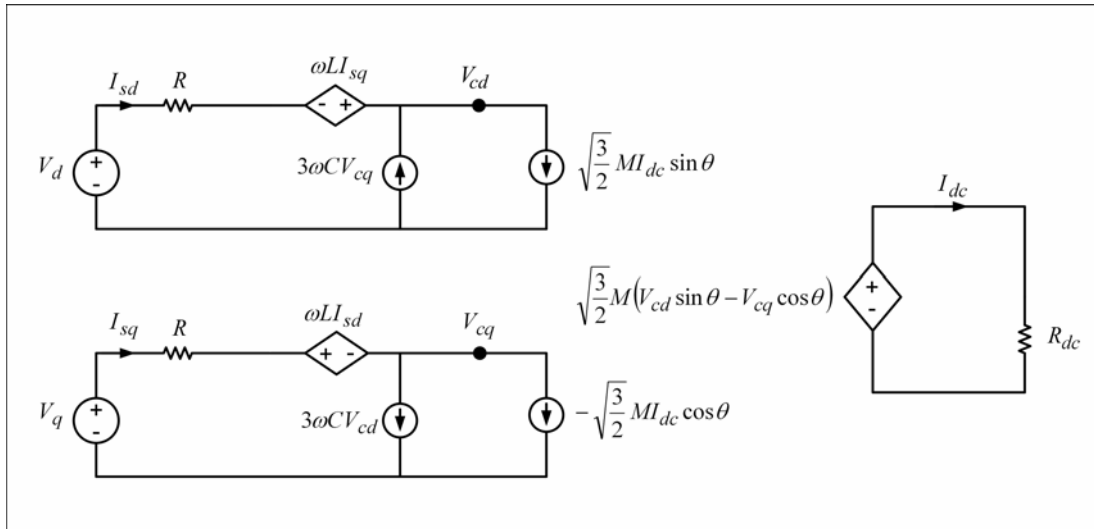
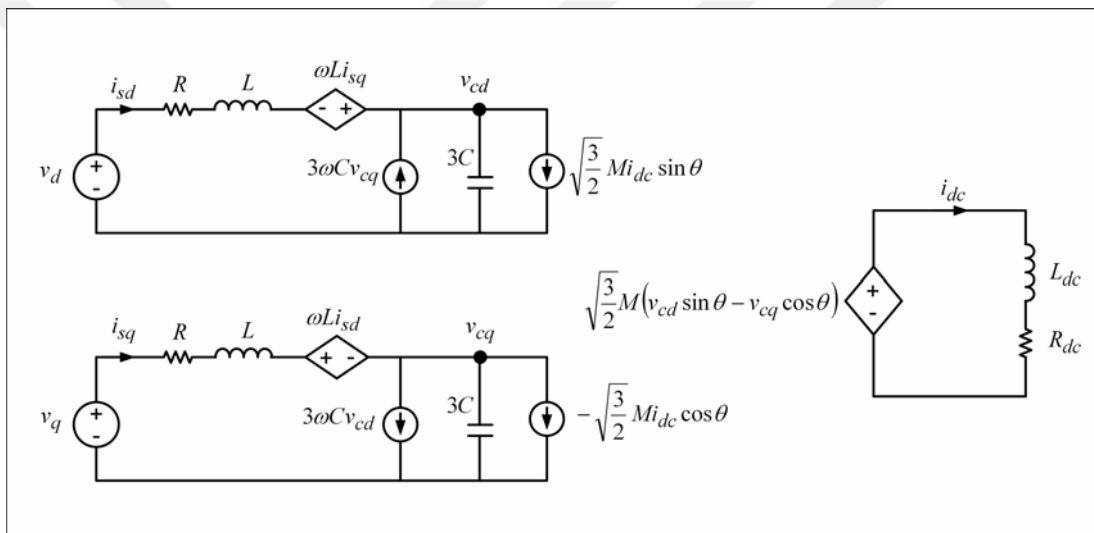


Figure 3.4: Equivalent circuit of CSC based STATCOM in abc-rotating frame.



(a)



(b)

Figure 3.5: Equivalent circuit of CSC based STATCOM in dq-stationary frame (a) for steady-state, (b) for transient-state.

The controlled input variables M_d and M_q are defined in (3.2) and (3.3) will be the re-arrangement of The state-space representation in (3.1).

$$\frac{d}{dt}x = \begin{bmatrix} -\frac{R}{L} & \omega & -\frac{1}{L} & 0 \\ -\omega & -\frac{R}{L} & 0 & -\frac{1}{L} \\ \frac{1}{3C} & 0 & 0 & \omega \\ 0 & \frac{1}{3C} & -\omega & 0 \end{bmatrix} x + \begin{bmatrix} 0 & 0 \\ 0 & 0 \\ \frac{1}{3C} & 0 \\ 0 & \frac{1}{3C} \end{bmatrix} u + \begin{bmatrix} \frac{1}{L} & 0 \\ 0 & \frac{1}{L} \\ 0 & 0 \\ 0 & 0 \end{bmatrix} w \quad (3.2)$$

$$y = \begin{bmatrix} 1 & 0 & 0 & 0 \\ 0 & 1 & 0 & 0 \end{bmatrix} x$$

Where $x = \begin{bmatrix} i_{sd} \\ i_{sq} \\ v_{cd} \\ v_{cq} \end{bmatrix}$, $u = \begin{bmatrix} M_d & i_{dc} \\ M_q & i_{dc} \end{bmatrix}$, $w = \begin{bmatrix} v_d \\ v_q \end{bmatrix}$

$$\begin{bmatrix} M_d \\ M_q \end{bmatrix} = \begin{bmatrix} \sqrt{\frac{3}{2}} M \sin \theta \\ -\sqrt{\frac{3}{2}} M \cos \theta \end{bmatrix} \quad (3.3)$$

The non-linearity is clear in CSC based STATCOM because of variety of state variables and controlled input variables that can be seen in the state-space representation in (3.3) [34]. Both input variables are depended by dc-link current and the d axis component has a cross-coupling with q component of the system [34]. The state feedback controller for CSC based STATCOM has these problems exactly. Therefore, the state-space model of CSC based STATCOM must be decoupled and linearized by accomplishing some few steps [22]. The reactive power of CSC based STATCOM can be controlled by applying pole-placement method via state feedback, decoupled and linearized state-space representation [33]. The state-feedback controller for the control system [21] as typical block diagram is shown in Fig.3.6. The d-axis component of the reference supply current can be produced by the outer loop of PI controller from the measured and reference dc-link current.

The required control input variables, M_d and M_q can be obtained by deducting the measured d and q-axis measured supply currents minus their reference values and the integrated error between them will be added to the state feedback.

Then, One of modulation techniques explained in Section 2.4 will be employed by the switching signal generator which utilizes these control variables for this purpose.

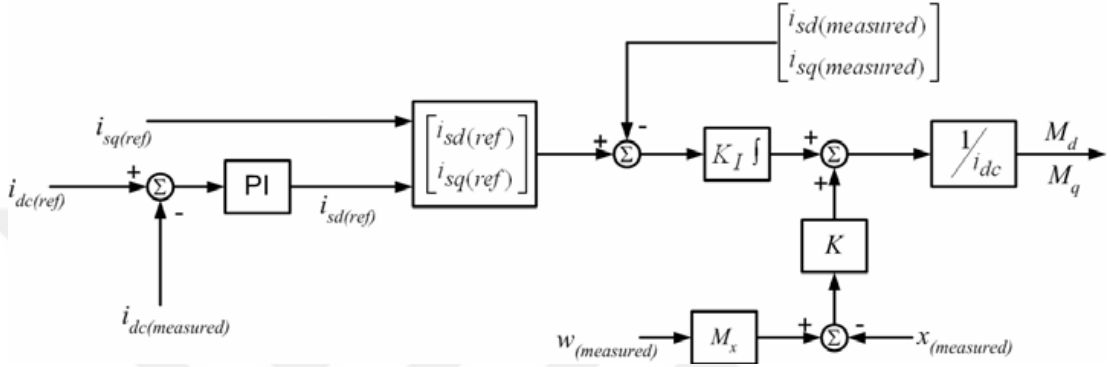


Figure 3.6: Typical block diagram of modern control method based on state feedback controller for CSC based STATCOM.

There is another state-space modeling for CSC based STATCOM can be depended instead of (3.1). The nonlinearity characteristic of CSC-based STATCOM controller because of i_{dc} part can be removed by utilizing the balance equation of active power as in.

$$P_{ac} = P_{dc} \Rightarrow -\frac{3V_d}{2n} I_{sd} = L_{dc} I_{dc} \frac{d}{dt} I_{dc} + R_{dc} I_{dc}^2 \quad (3.4)$$

After using power balance equation and mathematical calculation, the final equation will be as below.

$$\frac{d}{dt} (I_{dc}^2) = -\frac{2R_{dc}}{L_{dc}} (I_{dc}^2) - \frac{3V_d}{L_{dc}n} I_{sd} \quad (3.5)$$

By using (3.4) and (3.5), the final state-space modeling for CSC based STATCOM can be written as in.

$$\frac{d}{dt} \begin{bmatrix} i_{sd} \\ i_{sq} \\ v_{cd} \\ v_{cq} \\ i_{dc}^2 \end{bmatrix} = \begin{bmatrix} -\frac{R}{L} & -\omega & -\frac{1}{L} & 0 & 0 \\ \omega & -\frac{R}{L} & 0 & -\frac{1}{L} & 0 \\ \frac{1}{3C} & 0 & 0 & -\omega & 0 \\ 0 & \frac{1}{3C} & \omega & 0 & 0 \\ \frac{3V_d}{L_{dc}} & 0 & 0 & 0 & -\frac{R_{dc}}{L_{dc}} \end{bmatrix} * \begin{bmatrix} i_{sd} \\ i_{sq} \\ v_{cd} \\ v_{cq} \\ i_{dc}^2 \end{bmatrix} + \begin{bmatrix} 0 & 0 \\ 0 & 0 \\ \frac{1}{3C} & 0 \\ 0 & \frac{1}{3C} \\ 0 & 0 \end{bmatrix} \begin{bmatrix} M_d i_{dc} \\ M_q i_{dc} \end{bmatrix} + \begin{bmatrix} -\frac{1}{L} \\ 0 \\ 0 \\ 0 \\ 0 \end{bmatrix} V_d \quad (3.6)$$

Pole-Shifting Controller Design. The designing of this pole –placement controller depends on this state-space modeling. The desired outcomes of the system can be gotten by moving the poles of this system to desired poles position in pole placement technique [36]. Because of Eigen values control on the dynamic characteristics of the system outcomes and its relation poles position, these system poles are shifted. the system must be controllable for this method. In the dynamic modeling of systems, state-space equations involve three types of variables: state variables (x) and input (u) and output (y) variables with disturbance (e). So comparing (8) with the standard state-space representation, that is, The state variables (x), input (u) and output (y) variables with disturbance (e) are the parts of state-space equations in the dynamic modeling of systems. After comparing with the standard representation, it will be seen that.

$$\dot{x} = Ax + Bu + Fe, \quad (3.7)$$

$$y = Cx.$$

We get the system matrices as:

$$\begin{aligned} x &= [i_{sd} \quad i_{sq} \quad v_{cd} \quad v_{cq} \quad i_{dc}^2]^T; & u &= [M_d i_{dc} \quad M_q i_{dc}]^T; \\ e &= V_d; & y &= [i_q \quad i_{dc}^2]^T; \end{aligned} \quad (3.8)$$

$$A = \begin{bmatrix} -\frac{R}{L} & -\omega & -\frac{1}{L} & 0 & 0 \\ \omega & -\frac{R}{L} & 0 & -\frac{1}{L} & 0 \\ \frac{1}{3C} & 0 & 0 & -\omega & 0 \\ 0 & \frac{1}{3C} & \omega & 0 & 0 \\ \frac{3V_d}{L_{dc}} & 0 & 0 & 0 & -\frac{R_{dc}}{L_{dc}} \end{bmatrix}; \quad B = \begin{bmatrix} 0 & 0 \\ 0 & 0 \\ \frac{1}{3C} & 0 \\ 0 & \frac{1}{3C} \\ 0 & 0 \end{bmatrix};$$

$$C = \begin{bmatrix} 0 & 0 \\ 0 & 1 \\ 0 & 0 \\ 0 & 0 \\ 1 & 0 \end{bmatrix}^T; \quad F = \begin{bmatrix} -\frac{1}{L} \\ 0 \\ 0 \\ 0 \\ 0 \end{bmatrix}$$

In the above equations (3.7) five system states, two control inputs, and two control outputs are presented, where x is the state vector, u is the input vector, A is the basis matrix, B is the input matrix, and e is disturbance input.

If the controller is set as

$$u = -K * x + J * y_{ref} + N * e, \quad (3.9)$$

then the state equation of closed loop can be written as

$$\dot{x} = (A - B * K) * x + J * y_{ref} + B * N * e + F * e. \quad (3.10)$$

Here, for steady state condition:

$$x \cdot = 0. \quad (3.11)$$

Then,

$$y = C * (A - B * K)^{-1} * [B * J * y_{ref} + B * N * e + F * e] \quad (3.12)$$

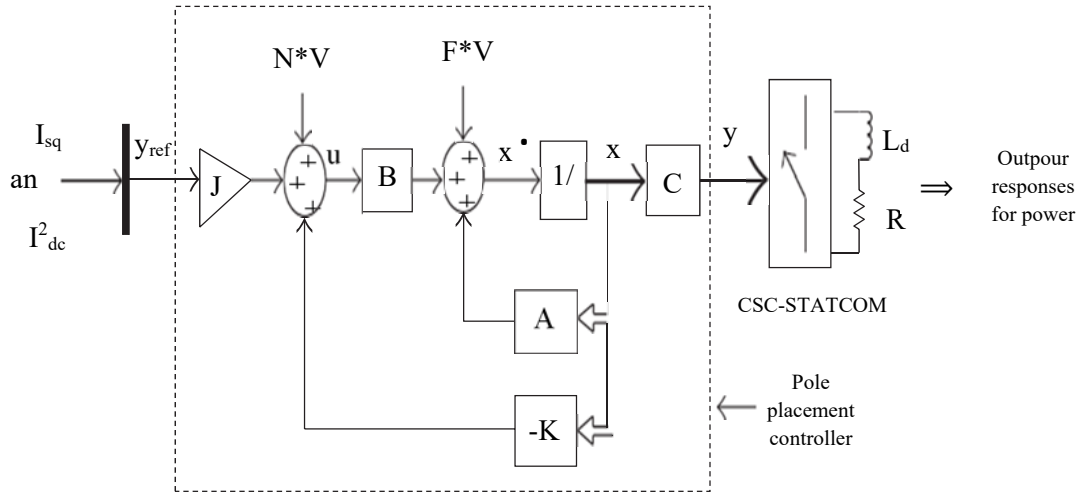


Figure 3.7: Control structure of pole placement controller based CSC-STATCOM.

where $J = (C * (- (A - B * K)^{-1} * B))^{-1}$ and $N = ((C * (-A + B * K))^{-1} * (C * (-A + B * K)^{-1} * F))$; these constant values are found out from a mathematical calculation for tracking the reference output value (y_{ref}) by the system output value (y). Here K is the state-feedback gain matrix. The gain matrix K is designed in such a way that (3.13) is satisfied with the desired poles:

$$|sI - (A - BK)| = (s - P_1)(s - P_2) \cdots (s - P_n) \quad (3.13)$$

where P_1, P_2, \dots, P_n are the desired pole locations. Equation (15) is the desired characteristic polynomial equation. The values of P_1, P_2, \dots, P_n are selected such that the system becomes stable and all closed-loop Eigenvalues are located in the left half of the complex-plane. The final configuration of the proposed pole-shifting controller based CSC-STATCOM is shown in Fig.3.7. The calculations of K, N and J matrices are implemented in Mat lab program and explained in Appendix B.

CHAPTER FOUR

SIMULATION AND DISCUSSION OF RESULTS

In this chapter, The circuit of power system will be described by their parameters values which is represented by two voltage sources and transmission line connect them together. Each source is equivalent to electrical power machine and step up transformer. The controlled STATCOM is connected at the middle point of the transmission line to divide the transmission line into two parts (TL1, TL2). Each part includes two circuit breakers (BK1, BK, BK3, BK4) for the two parts to protect the power system from the damage part. The parameters matrices of state space representation can be calculated to control the injected reactive power by CSC based STATCOM after disturbance cases. There are three disturbance cases applied to the system i) Three phase fault at transmission line (TL1) with applying two different loads at different periods at STATCOM bus ii) the same two different loads are connected to the STATCOM bus and suddenly disconnecting transmission line (TL1) from the service. iii) Three phase fault at transmission line (TL2) with applying two different loads at different periods at STATCOM bus. These cases will be simulated by Matlab program to apply the controlled CSC based STATCOM on the circuit and get better response in reactive power compensating at disturbance conditions.

4.1 Simulation Circuit

This circuit contains voltage source at sending end and another one at receiving end. There parameters are 500kV/3000MVA and 500kV/2500MVA respectively. The ratios of the internal reactance to the internal resistance for each source (X/R) are 8 and 7 respectively. The three voltages source for each three phase source are connected Y (star) to an internally grounded neutral. The length of each transmission

line is 300Km. The transmission line for three phase is a continuously transposed line. The positive and zero-sequence resistances are $[0.01755 \ 0.2758]$ ohms per unit length. The positive and zero-sequence inductances of transmission line are $[0.8737e-3 \ 3.220e-3]$ henries per unit length. The positive and zero-sequence capacitances of transmission line are $[13.33e-9 \ 8.297e-9]$ Farads per unit length. The magnitudes of the two large loads that are suddenly connected in different periods at STATCOM bus are (50 MW & 30 MVAR) and (100 MW & 50 MVAR) respectively. The load-1 and load-2 are connected to the bus through BK5 and BK6. The dc resistance (R_{dc}) and dc inductance (L_{dc}) of CSC based STATCOM = 0.01 ohm and 40 mH. The filter capacitance of CSC at AC side = 400 (micro) F. The equivalent resistance of Coupling transformer (R) for each phase = 0.3 ohm. The equivalent inductance of Coupling transformer (L) for each phase = 2mH. $\omega = 314$ and the frequency = 50 Hz. V_d (ref) = 1. System nominal voltage ($L-L$): 500 kV. The parameters matrices can be calculated from CSC based STATCOM parameters to depend them in the controller design. The simulated circuit and the subsystem are shown in Fig (4.1) and Fig (4.2). The simulation work of the circuit is done for discussing and getting the results in the following three cases:

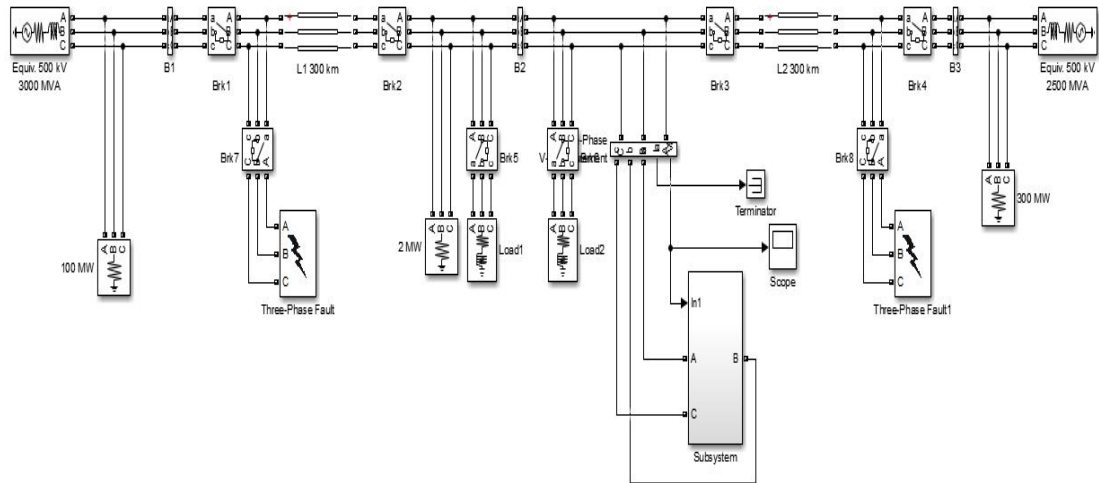


Figure 4.1: Simulation circuit with CSC-STATCOM connected to 2 sources 3 buses system test.

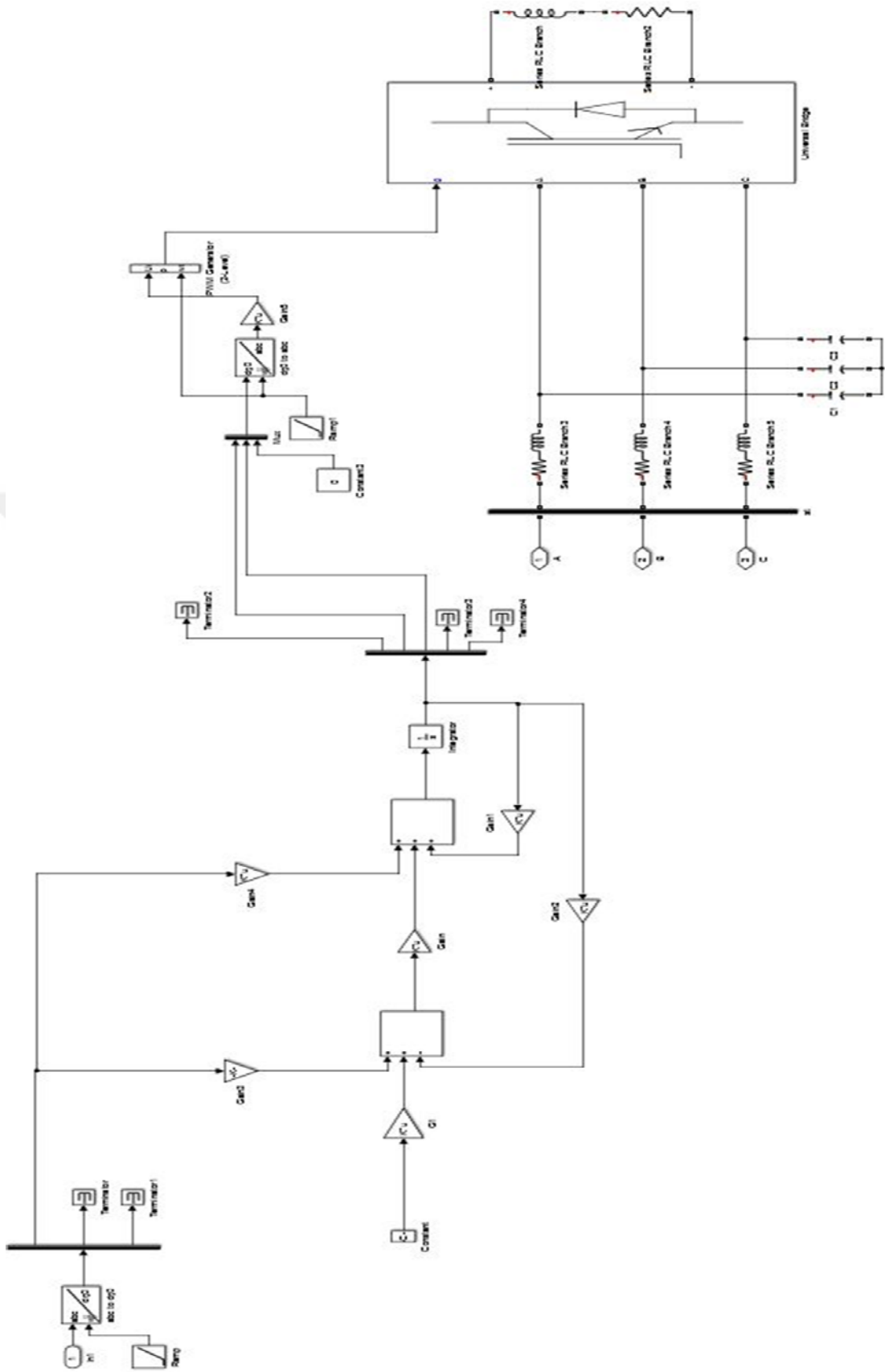


Figure 4.2: Subsystem of Pole Shifting Controller Based CSC-STATCOM.

I) Three phase fault at transmission line (TL1) with applying two different loads at different periods at STATCOM bus: The simulation of the circuit begins at $t = 0.0$ s and arrives to the end at $t = 1$ s. The load-1 (50 MW and 30 MVAR) and load-2 (100 MW and 50 MVAR) are not connected to the STATCOM bus at the beginning of the simulation (BK5 and BK6 are normally open). The bus voltage for each phase starts at 1 p.u in steady-state. The bus voltage for each phase is sinusoidal and the per unit value is gotten by dividing the rms value of this voltage on the base voltage of the system to look as constant magnitude at 1 p.u. Three phase fault block is connected to (TL1) at $t = 0.3$ second. The circuit breakers (BK1 and BK2) disconnects TL1 to isolate it from the system. Closing BK5 to link load-1 to the system at $t = 0.3$ second also. The voltage bus will fall from 1 p.u to stabilize at 0.94 p.u approximately without utilizing CSC-based STATCOM. It stays at this magnitude until $t = 0.65$ second where BK6 will close to link load-2 to the bus. This large load will cause another large reduction for this voltage to 0.864 p.u as shown in Fig (4.2).

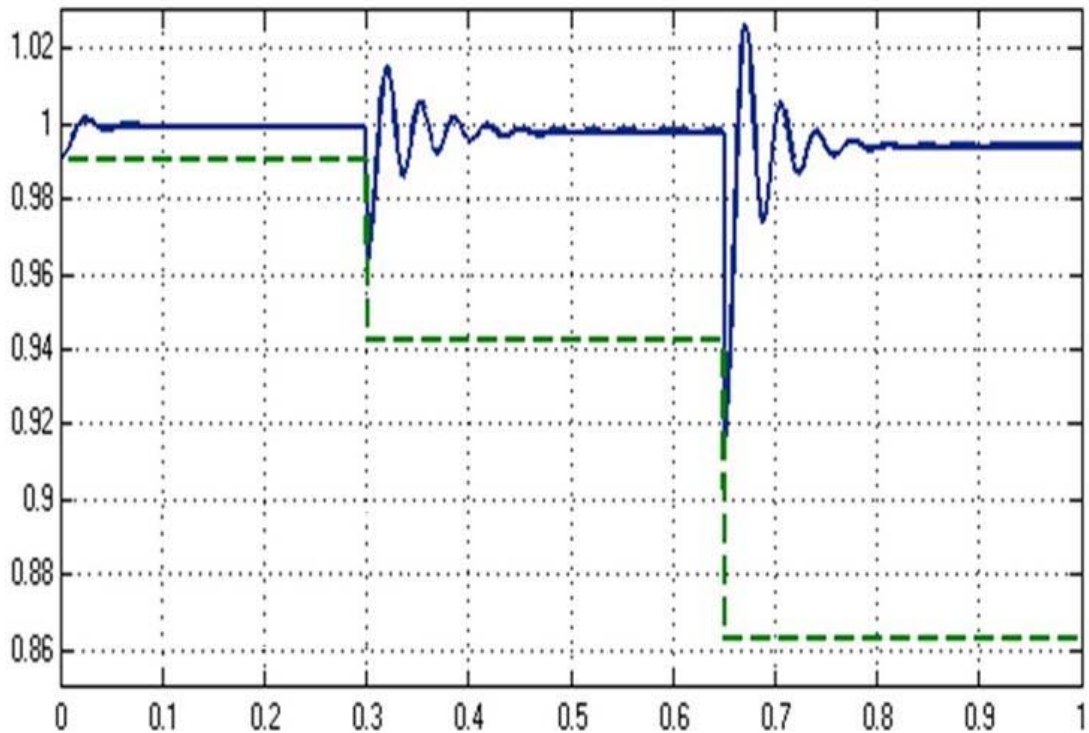


Figure 4.3: Bus voltages in p.u w.r.t. time without CSC-STATCOM and with CSC-STATCOM for the first case.

With the green intermittent line. The blue solid line in Fig (5) explains the voltage with using the CSC-STATCOM. At the steady state, there is no difference between the voltage of the STATCOM and bus voltage in the period from 0 s to 0.3 second. In this time the flowing of reactive and active between the bus and the STATCOM is zero. In this period, there is a small shift in the STATCOM voltage behind the bus voltage to compensate CSC losses, transformer and remain the reactor of the DC link side charged. The dc-link current is smoothly constant without changing in this period without changing in modulation index. The first disturbance period will cause the bus voltage to be less than CSC voltage. CSC based STATCOM will compensate this voltage by injecting the capacitive reactive power to raise this voltage to its main value. The fast response of pole placement controller to this disturbance makes the voltage to arrive to its normal value in 0.1 second. This response happens in few milliseconds. The time response of CSC in the second disturbance is longer than that of the first one. The damping oscillations of the voltage takes more time also. The active power won't flow from/to CSC at steady state period ($t = 0-0.3$ second) and (ϕ) equals zero. Connecting load-1 to the system makes the controller to response and discharge the DC reactor energy in the system direction between 0.3 and 0.65 second. The STATCOM will give active power to the system to meet the suddenly load (50 MW) with small oscillation for very short time. The load-2 entry (100 MW) Motivates the STATCOM to increase its active power to the bus with large oscillation and the power takes place time longer than that at the first load to stabilize at 600 KW. The active power will arrive to 600 KW to support the second source against the two large loads. The flowing of active power from CSC at the two loads periods are shown in Fig (4.3). The system bus absorbs 25 MVAR from 0 to 0.3 second. This mean, the STATCOM works in the capacitive mode at steady-state period. CSC will inject 70 MVAR when the bus exposes to the load (30 MVAR) with small oscillation for very short time at ($t = 0.3$ second). The capacitive reactive power injecting will raise to 180MVAR at ($t = 0.65$ second) with connecting the second load as explained in Fig (4.4). The reactive power is selected by controlling the input variables (M_d and M_q) to get the desired MVAR. The oscillation and damping time depends on the load magnitude and the poles positions to make the system more stability.

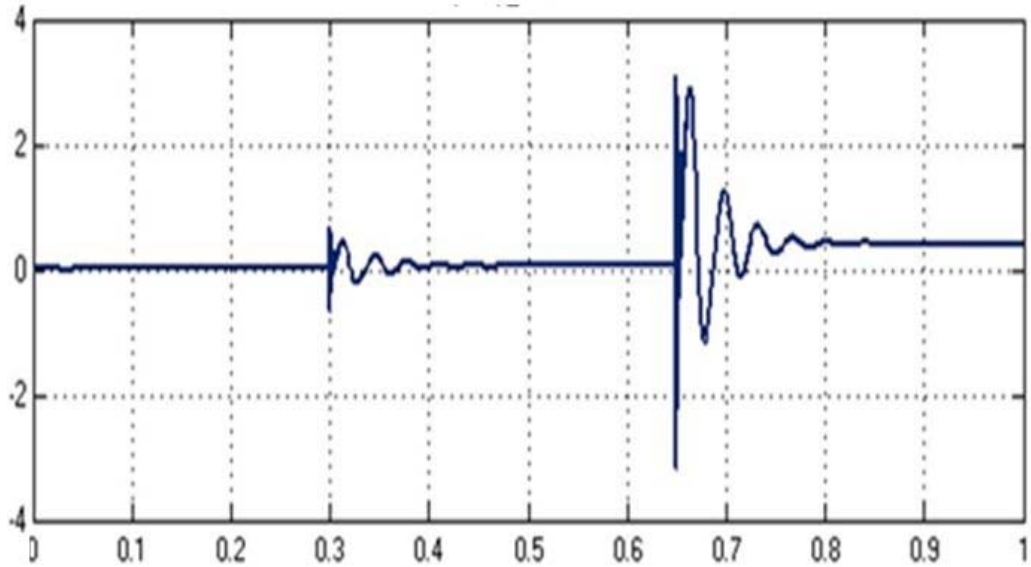


Figure 4.4: Active power of CSC-STATCOM in MW w.r.t. time for the first case.

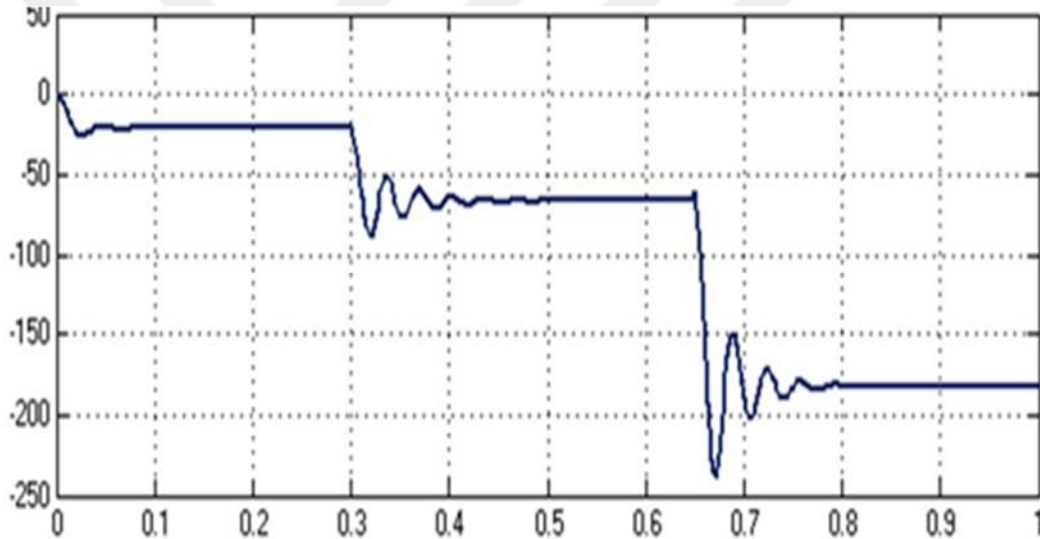


Figure 4.5: Reactive power of CSC-STATCOM in MVAR w.r.t. time for the first case.

II) The same two different loads are connected to the STATCOM bus and suddenly disconnecting transmission line (TL1) from the service: The simulation will take place 1 second from the beginning to the end. In this case, The load-1 (50 MW and 30 MVAR) and load-2 (100 MW and 50 MVAR) are connected to the STATCOM bus at the beginning of the simulation (BK5 and BK6 are normally closed). The bus voltage for each phase starts at 0.936 p.u in steady-state. The bus voltage for each phase is sinusoidal and the per unit value is gotten by dividing the rms value of this voltage on the base voltage of the system to look as constant magnitude at 0.936p.u. Three phase fault block is connected to (TL1) at $t = 0.4$

second. The circuit breakers (BK1 and BK2) disconnects TL1 to isolate it from the system. Closing BK7 makes The voltage bus to fall from 0.936 p.u to stabilize at 0.864p.u approximately without utilizing CSC-based STATCOM as shown in Fig (4.5).

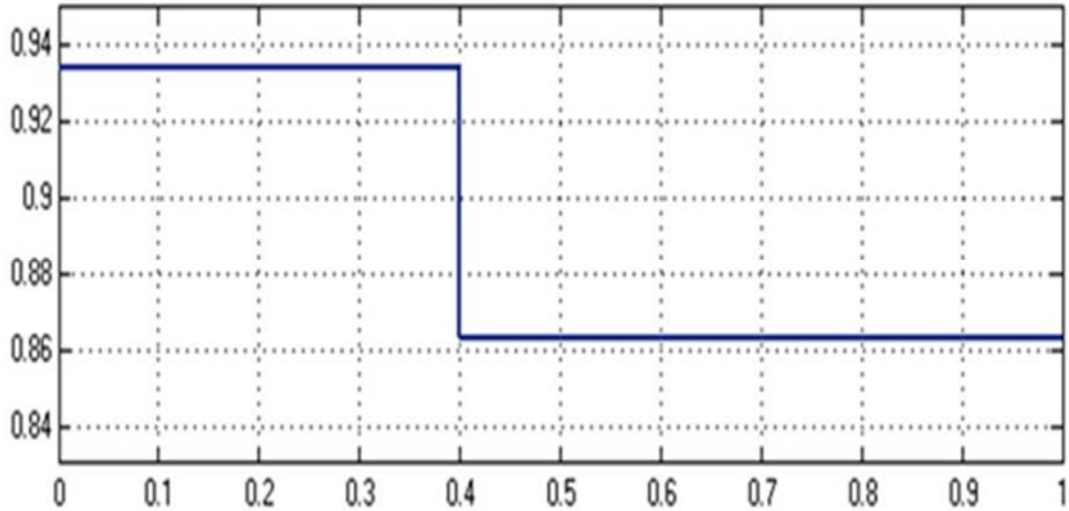


Figure 4.6: Bus voltages in p.u w.r.t. time without CSC-STATCOM for the second case.

The blue solid line in Fig (4.6) explains the voltage with using the CSC-STATCOM. At the steady state, the voltage will be stable at 0.995 p.u. This mean, CSC addition voltage to the bus until 0.4 second. In this time the flowing of reactive and active between the bus and the STATCOM is not zero because of connecting load-1 and load-2 from simulation start. The dc-link current is smoothly constant without changing in this period without changing in modulation index. The disturbance period will cause the bus voltage to be less than CSC voltage. CSC based STATCOM will compensate this falling by increasing the injected reactive power to raise this voltage to its main value. The fast response of pole placement controller to this disturbance makes the voltage to arrive to its normal value in 0.1 second. This response happens in few milliseconds. The time response of CSC in the disturbance case is very short. The damping oscillations of the voltage takes a little time.

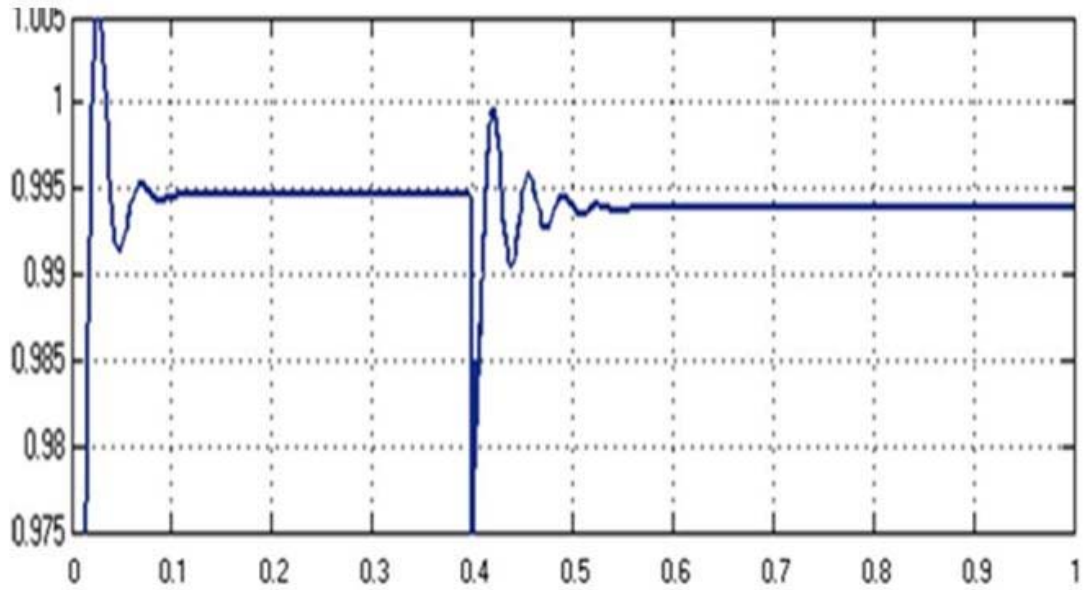


Figure 4.7: Bus voltage in p.u w.r.t. time with CSC-STATCOM for the second case.

A small active power (300 KW approximately) will flow from CSC at steady state period ($t = 0-0.4$ second) and (ϕ) won't equal zero. Closing BK7 of the fault block or disconnecting BK1 and BK2 to isolate TL1 from the system makes the controller to response and increase the discharging of the DC reactor energy in the system direction between after $t = 0.4$ second. The STATCOM will increase its active power to the system to beat on the suddenly disturbance with small oscillation for very short time at 1 MW approximately. This increasing is happened with oscillations and damping time 0.1 second to support the second source against the disturbance. The flowing of active power from CSC at the disturbance are shown in Fig (4.7).

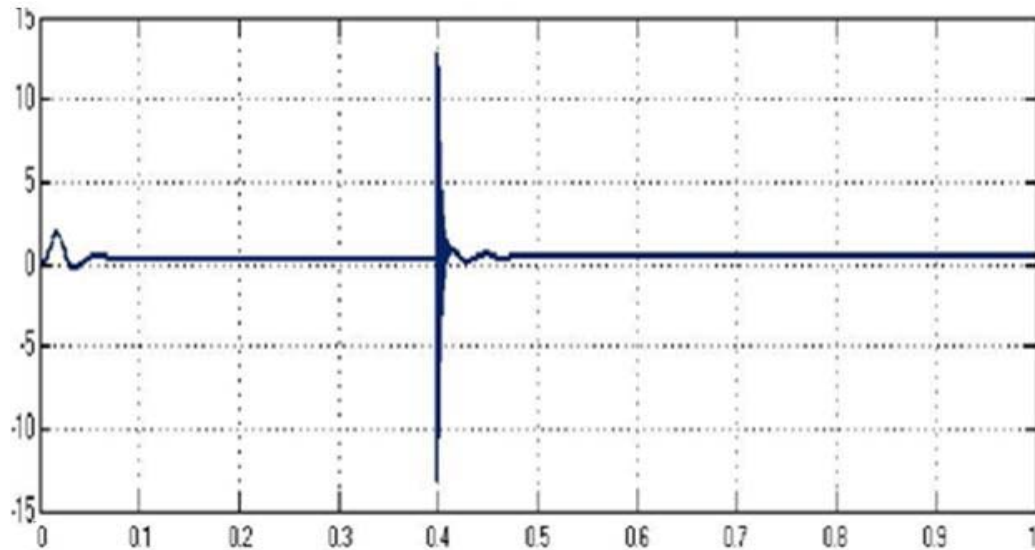


Figure 4.8: Active power of CSC-STATCOM in MW w.r.t. time for the second case.

The system bus absorbs 160 MVAR from 0 to 0.4 second. This mean, the STATCOM works in the capacitive mode at steady-state period. CSC will inject addition 24 MVAR when the bus exposes to the disturbance with small oscillation for very short time at ($t = 0.4$ second). The capacitive reactive power injecting will raise to 184 MVAR with connecting the fault block as explained in Fig (4.8). The reactive power is selected by controlling the input variables (M_d and M_q) to get the desired MVAR. The oscillation and damping time depends on the load magnitude and the poles positions to make the system more stability.

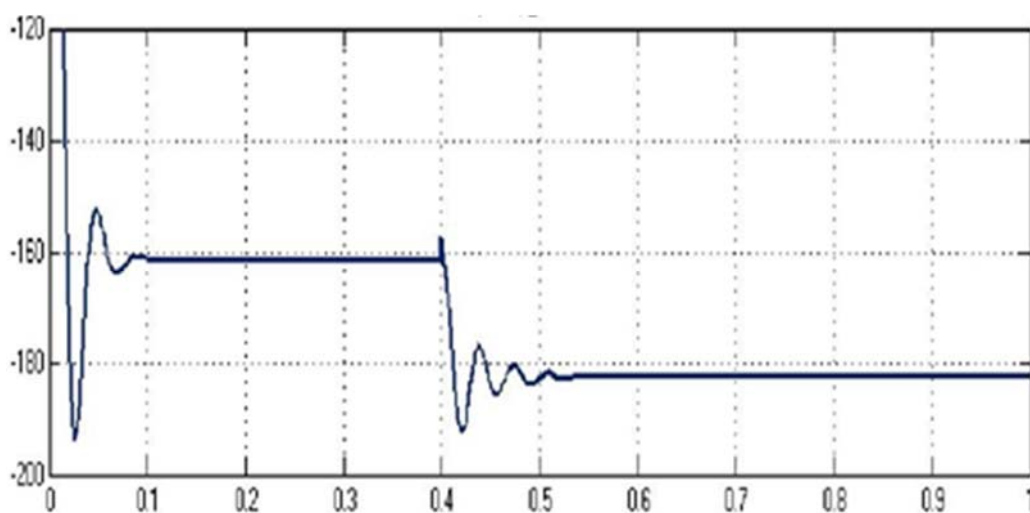


Figure 4.9: Reactive power of CSC-STATCOM in MVAR w.r.t. time for the second case.

III) Three phase fault at transmission line (TL2) with applying two different loads at different periods at STATCOM bus: The simulation of the circuit begins at $t = 0.0$ s and arrives to the end at $t = 1$ s. The load-1 (50 MW and 30 MVAR) and load-2 (100 MW and 50 MVAR) are not connected to the STATCOM bus at the beginning of the simulation (BK5 and BK6 are normally open). The bus voltage for each phase starts at 0.99p.u in steady-state. The bus voltage for each phase is sinusoidal and the per unit value is gotten by dividing the rms value of this voltage on the base voltage of the system to look as constant magnitude at 0.99 p.u. Three phase fault block is connected to (TL2) at $t = 0.4$ second. The circuit breakers (BK3 and BK4) disconnects TL2 to isolate it from the system. Closing BK5 to link load-1 to the system at $t = 0.4$ second also. The voltage bus will fall from 0.99p.u to stabilize at 0.956p.u approximately without utilizing CSC-based STATCOM. It stays at this magnitude until $t = 0.7$ second where BK6 will close to link load-2 to the bus. This large load will cause another large reduction for this voltage to 0.896 p.u as shown in Fig (4.9) with the green intermittent line.

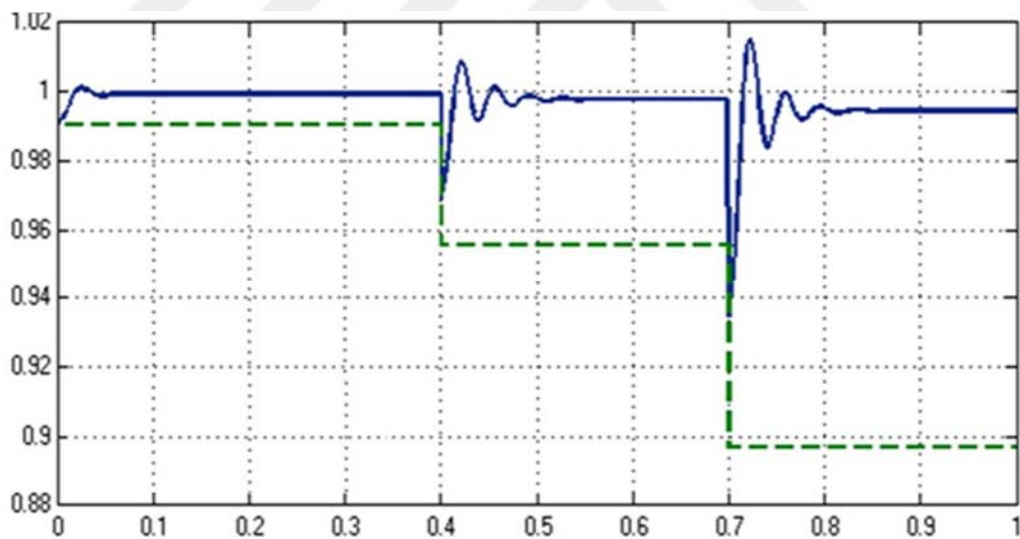


Figure 4.10: Bus voltages in p.u w.r.t. time without CSC-STATCOM and with CSC- STATCOM for the third case.

The blue solid line in Fig (4.9) explains the voltage with using the CSC-STATCOM. At the steady state, there is a small difference between the voltage of the STATCOM and bus voltage in the period from 0 s to 0.4 second. In this time the flowing of reactive and active between the bus and the STATCOM is low. In this period, there is a small shift in the STATCOM voltage behind the bus voltage to

compensate CSC losses, transformer and remain the reactor of the DC link side charged. The dc-link current is smoothly constant without changing in this period without changing in modulation index. The first disturbance period will cause the bus voltage to be less than CSC voltage. CSC based STATCOM will compensate this voltage by injecting the capacitive reactive power to raise this voltage to its main value. The fast response of pole placement controller to this disturbance makes the voltage to arrive to its normal value in 0.1 second. This response happens in few milliseconds. The time response of CSC in the second disturbance is longer than that of the first one. The damping oscillations of the voltage takes more time also.

A small active power will flow from CSC at steady state period ($t = 0-0.4$ second) and (φ) won't equals zero. Connecting load-1 to the system makes the controller to response and discharge the DC reactor energy in the system direction between 0.4 and 0.7 second. The STATCOM will give active power to the system to meet the suddenly load (50 MW) with small oscillation for very short time. The load-2 entry (100 MW) Motivates the STATCOM to increase its active power to the bus with large oscillation and the power takes place time longer than that at the first load to stabilize at 200 KW. The active power will arrive to 200 KW to support the first source against the two large loads. The flowing of active power from CSC at the two loads periods are shown in Fig (4.10).

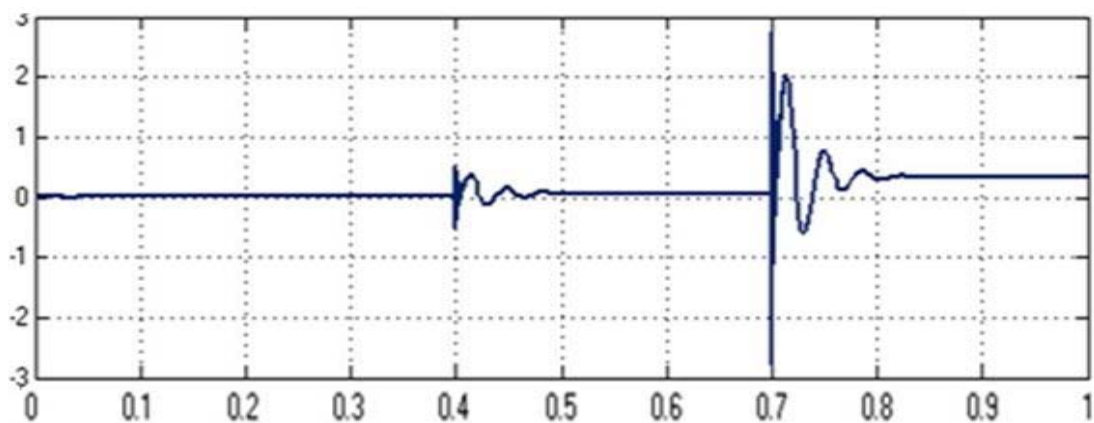


Figure 4.11: Active power of CSC-STATCOM in MW w.r.t. time for the third case.

The system bus absorbs 20 MVAR from 0 to 0.4 second. This mean, the STATCOM works in the capacitive mode at steady-state period. CSC will inject 70 MVAR when the bus exposes to the load (30 MVAR) with small oscillation for very

short time at ($t = 0.4$ second). The injecting of capacitive reactive power will raise to 170 MVAR at ($t = 0.7$ second) with connecting the second load as explained in Fig (4.11). The reactive power is selected by controlling the input variables (M_d and M_q) to get the desired MVAR. The oscillation and damping time depends on the load magnitude and the poles positions to make the system more stability.

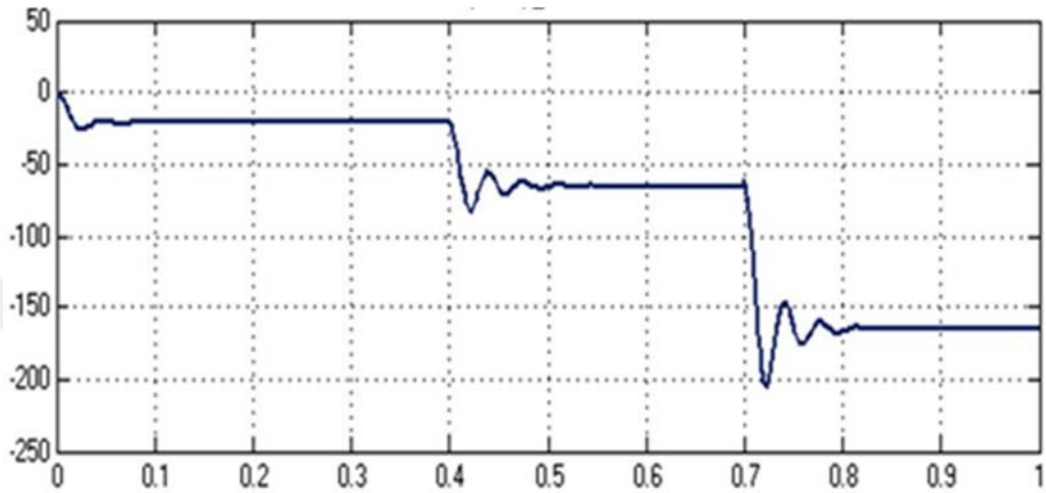


Figure 4.12: Reactive power of CSC-STATCOM in MVAR w.r.t. time for the third case.

CHAPTER FIVE

CONCLUSIONS AND SUGGESTIONS FOR FUTURE WORK

5.1 Conclusions

In this work, it can be seen that the basic arrangement of the Current source converter circuit is reviewed. The AC side and DC side of CSC has been described with presenting the AC outputs before and after the filter. The output three phase currents of CSC have pulses in the positive and negative parts because of the harmonics content in addition to the fundamental wave of the currents. These main currents have the same frequency of the system. The harmonic content can be absorbed by connecting a capacitive filter after power electronic switches to prevent the harmonic pulse currents from passing to the system bus. Only the fundamental wave of each phase current will pass. There is shift angle (θ) between the line current and line-to-line voltage. If this angle between $0 \leq \theta \leq \pi/2$, CSC generates inductive reactive power in the inductive mode and produces capacitive reactive power if its position between $\pi/2$ and π . The reactive power can be controlled by varying (ϕ) to inject it or absorb the desired value by depending on the disturbance situation of power system. SPWM technique is one of the popular methods that can be utilized to power electronic switches of CSC-STATCOM. The modern control requires transforming the differential equations of CSC from abc-rotating frame to 0dq-stationary frame for both sides (AC and DC). This will transfer the abc alternating values into two constant values. The proposed method depends on pole shifting controller to control on Md and Mq (modulation index in 0dq frame) to get the required reactive power with fast response after disturbance conditions. The gain matrix K is calculated according to (3.13) by selecting the desired pole locations.

The study outlined the following conclusions:

- _ When CSC based STATCOM is used, a significant improvement in power quality for the system is obtained at different disturbance conditions.
- _ The use of proposed modern control with CSC based STATCOM gave interesting results and good response for any change in the power system.
- _ The study shows that the reactive power generated CSC based STATCOM increases or decreases by the increasing or decreasing the inductive load in power system.
- _ The results proved that CSC has quick starting, high converter reliability, small filtering requirements compared with VSC case because of the low switching frequency and inherent short-circuit protection.

5.2 Future work

In future work, The sample system modulation by MATLAB Simulink with all power system components can be done. The neural network control of the reactive power injected with any disturbance can be used. Furthermore, the possibility of utilizing neuro-fuzzy controllers to control the reactive power of CSC and improve the power quality of the power system can be studied. The advantage of fuzzy controller and adaptability nature of artificial neural networks can be combined for this purpose. the reactive power compensation by FPGA and DSP chips can be also investigated.

REFERENCES

- [1] A. Ghosh and G. Ledwich, Power Quality Enhancement Using Custom Power Devices, *Kluwer Academic Publishers*, 2002
- [2] IEEE Std. 1159-1995, "IEEE Recommended Practice for Monitoring Electric Power Quality"
- [3] N.G. Hingorani and L. Gyugyi, Understanding FACTS, *IEEE Press*, New York, 1999
- [4] J. Dixon, L. Moran, J. Rodriguez, R. Domke, "Reactive Power Compensation Technologies, State-of-the-Art Review", *Proceedings of the IEEE*, vol.93, pp.2144-2164, Dec.2005
- [5] C. Schauder, *et.al.*, "Development of a ± 100 MVAr Static Condenser for Voltage Control of Transmission Systems", *IEEE Tran. on Power Delivery*, vol.10, no.3, pp.1486-1496, July 1995
- [6] S. Mori, K. Matsuno, *et.al.*, "Development of a Large Static VAR Generator Using Self-Commutated Inverters for Improving Power System Stability", *IEEE Tran. on Power Systems*, vol. 8, no. 1, pp. 371-376, Feb. 1993
- [7] L. Moran, P. Ziogas, G. Joos, "Analysis and Design of a Three-Phase Current Source Solid-State Var Compensator", *IEEE Tran. Ind. Appl.*, vol.25, no.2, March/April 1989
- [8] Bin Wu, "High-Power Converters and AC Drives", *IEEE Press*, 2006
- [9] H. Stemmler, "High Power Industrial Drives", *Proceedings of IEEE*, August 1994
- [10] H.F. Bilgin, K.N.Kose, G. Zenginobuz, M. Ermis, E. Nalcaci, I. Cadirci, H. Kose, "A unity-power-factor buck-type PWM rectifier for medium/high-power DC motor drive applications", *IEEE Tran. on Ind. Appl.* vol.38,no.5,pp.1412-1425,Sept-Oct. 2002

- [11] S. Nonaka, Y. Neba, "A PWM GTO Current Source Converter-Inverter System with Sinusoidal Input and Outputs", IEEE Tran. Ind. Appl., vol.25, no.1, Jan/Feb. 1989
- [12] Y. Xiao, B. Wu, F. De Winter, R. Sotudeh, "High Power GTO AC/DC Current Source Converter with Minimum Switching Frequency and Maximum Power Factor", Canadian Conf. Electrical and Computer Engineering, vol.1, pp.331- 334, Sept. 1996
- [13] N. Zargari, Y. Xiao, B.Wu, "A Near Unity Input Displacement Factor for Medium Voltage CSI Based AC Drives", Applied Power Electronics Conference and Exposition, Feb. 1997
- [14] J. Rodriguez, J. Pont, N. Becker and A. Weinstein, "Regenerative Drives in the Megawatt Range for High-Performance Downhill Belt Coveyors", IEEE Trans. Ind. Appl., vol.38, no.1, Jan/Feb. 2002
- [15] A. Weber, E. Carroll, M. Frecker, "IGCTs for Induction Heating", PCIM, Nuremberg, May, 2002
- [16] C. Namuduri, P.C. Sen, "Optimal pulse width modulation for current source inverters", IEEE Tran. Ind. Appl., vol.IA-22, no.6, pp.1052-1072, Nov/Dec. 1986
- [17] J.C. Wiseman, B. Wu, "Active Damping Control of a High Power PWM Current Source Rectifier for Line Current THD Reduction", IEEE Tran. Ind. Electr., vol.52, no.3, June 2005
- [18] H.F. Bilgin, M. Ermis, et.al, "Reactive Power Compensation of Coal Mining Excavators by using a new generation STATCOM", IEEE Tran. on Ind. Appl. vol.43,no.1,pp.97-110, Jan-Feb. 2007
- [19] Wang BS, Cathey JJ, "DSP-controlled, Space-Vector PWM, Current Source Converter for STATCOM application", Elect. Pow. Syst. Res., vol.67, no.2, pp. 123-131, Nov 2003
- [20] B.M. Han, S.I. Moon, "Static Reactive Power Compensator Using Soft-Switching Current-Source Inverter", IEEE Tran. Ind. Electr., vol.48, no.6, Dec.2001.
- [21] D. Shen, P.W. Lehn, "Modeling, Analysis, and Control of a Current Source Inverter-Based STATCOM", IEEE Tran. Power Delivery, vol.17, no.1, Jan. 2002

- [22] Y. Ye, M. Kazerani, V. H. Quintana, "Current-Source Converter Based STATCOM: Modeling and Control", IEEE Tran. Power Delivery, vol.20.,no. 2, April 2005
- [23] M. Kazerani, Y. Ye, "Comparative Evaluation of Three-Phase PWM Voltage- and Current- Source Converter Topologies in FACTS Applications", IEEE PES Summer Meeting, vol.1, pp.473-479,2002
- [24] H.R. Kashenas, A. Abdolahi, "Analysis of a Voltage Regulator for Self-excited induction generator employing Current-type Static Compensator", Canadian Conference on Electrical and Computer Engineering, vol.2, pp.1053-1058, May 2001
- [25] Zhenxue Xu, "Advance Semiconductor Device and Topology for High Power Current Source Converter", Ph.D. Thesis, Electrical Engineering, Virginia Polytechnic Institute and State University, December 2003.
- [26] IEEE Std. 519-1992, "IEEE Recommended Practices and Requirements for Harmonic Control in Electrical Power Systems", 1993
- [27] S. Hiti, V. Vlatkovic, D. Borojevic, F.C.Y. Lee, "A New Control Algorithm for Three-Phase PWM Buck Rectifier with Input Displacement Factor Compensation", IEEE Tran. Power Electr., vol.9,no.2, March 1994
- [28] H.R. Karshenas, H.A. Kojori, S.B. Dewan, "Generalized Techniques of Selective Harmonic Elimination and Current Control in Current Source Inverters/Converters", vol.10, no.5, IEEE Tran. Power Elect., Sept. 1995
- [29] V. Vlatkovic, D. Borojevic, "Digital-Signal-Processor-Based Control of Three-Phase Space Vector Modulated Converters", IEEE Trans. Ind. Elect., vol.41, no.3, June, 1994
- [30] J.R. Espinoza, G. Joos, J.I. Guzman, L.A. Moran, R.P. Burgos, "Selective Harmonic Elimination and Current/Voltage Control in Current/Voltage Source Topologies: A unified Approach", IEEE Tran. Ind. Electr., vol.48,no.1, Feb. 2001
- [31] J. Espinoza, G. Joos, H.Jin, "DSP Based Space Vector PWM Pattern Generators for Current Source Rectifiers and Inverters", Canadian Conf. Electrical and Computer Engineering, vol.2, pp.979-982, Sept. 1995.

- [32] M. Salo, H. Tuusa, "A Vector Controlled Current-Source PWM Rectifier with a Novel Current Damping Method", IEEE Tran. Power Electr., vol.15, no.3, May,2000.
- [33] K. Ogata, "Modern Control Engineering", Prentice-Hall International Inc., USA, 1990.
- [34] J. Espinoza, G. Joos, "State Variable Decoupling and Power Flow Control in PWM Current Source Rectifier", IEEE Tran. Ind. Electr., Feb. 1998
- [35] Bin Wu, "High-Power Converters and AC Drives", IEEE Press, 2006
- [36] S. Gupta and R. K. Tripathi, "Transient stability assessment of two-area power system with robust controller based CSC-STATCOM," *Journal of Control Engineering and Applied Informatics*, vol. 16, no. 3, pp. 3–12, 2014.
- [37] S. Gupta and R. K. Tripathi, "FACTS modelling and control: Application of CSC based STATCOM in transmission lines," Engineering and Systems (SCES), 2012 Students Conference on. IEEE, 2012.

APPENDIX

Appendix-A : Modeling of Current Source Converter Based Statcom in DQ Stationary Frame	56
Appendix-B : Calculations of K, J and N Matrices.....	64



Appendix A: Modeling of Current Source Converter Based Statcom in DQ Stationary Frame

CSC based STATCOM will be modeled in dq-stationary frame for balanced AC supply. For modeling, the equivalent circuit shown in Fig.A.1 will be used. In this circuit, three phase delta connected filter capacitor bank is connected in wye and equivalent capacitance of each capacitor is taken as $3C$. Following assumptions will be considered in the modeling:

1. all the power semiconductor switches are lossless
2. three phase balanced AC supply having harmonic-free line voltages, as defined in (A.1).

$$\left. \begin{aligned} v_R &= V \cos(\omega t) \\ v_S &= V \cos(\omega t - 2\pi/3) \\ v_T &= V \cos(\omega t - 4\pi/3) \end{aligned} \right\} \quad (\text{A.1})$$

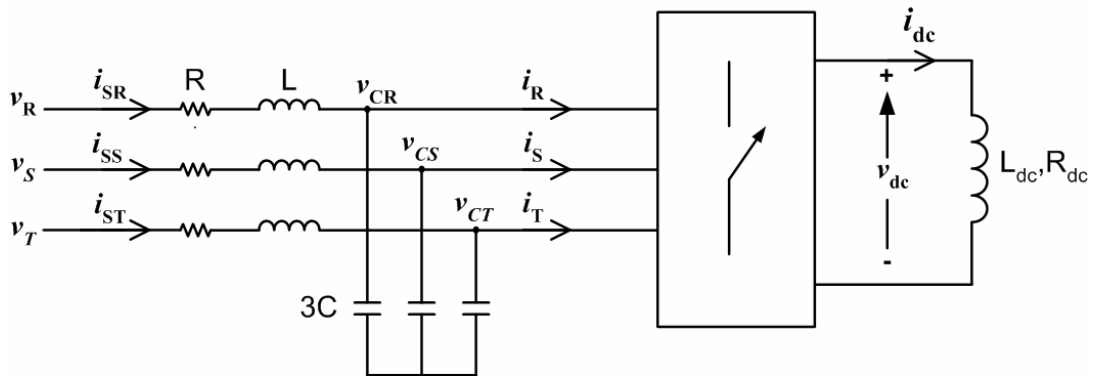


Figure A.1: Circuit diagram of CSC based STATCOM to be used for modeling.

AC side differential equations are given in (A.2) for phase R. Same equations can be easily written for the other phases, S and T.

$$\left. \begin{aligned} v_R &= Ri_{SR} + L \frac{di_{SR}}{dt} + v_{CR} \\ i_{SR} &= 3C \frac{dv_{CR}}{dt} + i_R \end{aligned} \right\} \quad (\text{A.2})$$

DC side differential equation of CSC based STATCOM is as follows

$$v_{dc} = L_{dc} \frac{di_{dc}}{dt} + R_{dc} i_{dc} \quad (\text{A.3})$$

AC side and DC side quantities are coupled with switching functions as in (A.4).

$$\left. \begin{aligned} v_{dc} &= (m_1 - m_2)v_{CR} + (m_3 - m_4)v_{CS} + (m_5 - m_6)v_{CT} \\ i_R &= (m_1 - m_2)i_{dc} \\ i_S &= (m_3 - m_4)i_{dc} \\ i_T &= (m_5 - m_6)i_{dc} \end{aligned} \right\} \quad (\text{A.4})$$

Using (2.2), (2.3) and (2.4), these switching functions can be expressed in terms of their Fourier components as in (A.5).

$$\left. \begin{aligned} m_1 - m_2 &= M \sin(\omega t + \theta) + b_h \sin(\omega_h t - \lambda) \\ m_3 - m_4 &= M \sin(\omega t + \theta - 2\pi/3) + b_h \sin(\omega_h t - \xi) \\ m_5 - m_6 &= M \sin(\omega t + \theta - 4\pi/3) + b_h \sin(\omega_h t - \psi) \end{aligned} \right\} \quad (\text{A.5})$$

Switching functions do not linearly dependent on the control variables modulation index, M and phase angle, θ since they contain harmonic components, which do not depend on modulation index and phase angle explicitly.

In order to linearize the switching functions harmonic components should be neglected. This does not cause any problem in analyzing the system performance since harmonics do not contribute to active and reactive power flow. Then, switching functions can be approximated as in (A.6).

$$\begin{aligned}
m_1 - m_2 &= M \sin(\omega t + \theta) \\
m_3 - m_4 &= M \sin(\omega t + \theta - 2\pi/3) \\
m_5 - m_6 &= M \sin(\omega t + \theta - 4\pi/3)
\end{aligned} \tag{A.6}$$

Before applying transformation from *abc*-rotating frame to *0dq*-stationary frame, (A.2) and (A.4) must be rearranged and put into appropriate matrix form as in (A.7), (A.8) and (A.9)

$$\begin{bmatrix} v_R \\ v_S \\ v_T \\ i_R \\ i_S \\ i_T \end{bmatrix} = \begin{bmatrix} L_{P+R} & 0 & 0 & 1 & 0 & 0 \\ 0 & L_{P+R} & 0 & 0 & 1 & 0 \\ 0 & 0 & L_{P+R} & 0 & 0 & 1 \\ 1 & 0 & 0 & -3C_p & 0 & 0 \\ 0 & 1 & 0 & 0 & -3C_p & 0 \\ 0 & 0 & 1 & 0 & 0 & -3C_p \end{bmatrix} \begin{bmatrix} i_{SR} \\ i_{SS} \\ i_{ST} \\ v_{CR} \\ v_{CS} \\ v_{CT} \end{bmatrix} \tag{A.7}$$

Where $p=d/dt$

$$v_{dc} = [M \sin(\omega t + \theta) \quad M \sin(\omega t + \theta - 120^\circ) \quad M \sin(\omega t + \theta - 240^\circ)] \begin{bmatrix} v_{CR} \\ v_{CS} \\ v_{CT} \end{bmatrix} \tag{A.8}$$

$$\begin{bmatrix} i_R \\ i_S \\ i_T \end{bmatrix} = \begin{bmatrix} M \sin(\omega t + \theta) \\ M \sin(\omega t + \theta - 120^\circ) \\ M \sin(\omega t + \theta - 240^\circ) \end{bmatrix} [i_{dc}] \tag{A.9}$$

Transformation takes place first from *abc*-rotating frame to $0\alpha\beta$ -rotating frame, then to *0dq*-stationary frame. These are done by proper transformation matrices. These transformation matrices are derived referring to Fig.A.2 as in (A.10)- (A.13).

$$\begin{bmatrix} a \\ b \\ c \end{bmatrix} = C_1 \begin{bmatrix} 0 \\ \alpha \\ \beta \end{bmatrix} = \sqrt{\frac{2}{3}} \begin{bmatrix} 1/\sqrt{2} & 1 & 0 \\ 1/\sqrt{2} & -1/2 & \sqrt{3}/2 \\ 1/\sqrt{2} & -1/2 & -\sqrt{3}/2 \end{bmatrix} \begin{bmatrix} 0 \\ \alpha \\ \beta \end{bmatrix} \tag{A.10}$$

$$\begin{bmatrix} 0 \\ \alpha \\ \beta \end{bmatrix} = C_2 \begin{bmatrix} 0 \\ d \\ q \end{bmatrix} = \begin{bmatrix} 1 & 0 & 0 \\ 0 & \cos \omega t & -\sin \omega t \\ 0 & \sin \omega t & \cos \omega t \end{bmatrix} \begin{bmatrix} 0 \\ d \\ q \end{bmatrix} \quad (\text{A.11})$$

$$C_1 = \sqrt{\frac{2}{3}} \begin{bmatrix} 1/\sqrt{2} & 1 & 0 \\ 1/\sqrt{2} & -1/2 & \sqrt{3}/2 \\ 1/\sqrt{2} & -1/2 & -\sqrt{3}/2 \end{bmatrix} \quad (\text{A.12})$$

$$C_2 = \begin{bmatrix} 1 & 0 & 0 \\ 0 & \cos \omega t & -\sin \omega t \\ 0 & \sin \omega t & \cos \omega t \end{bmatrix} \quad (\text{A.13})$$

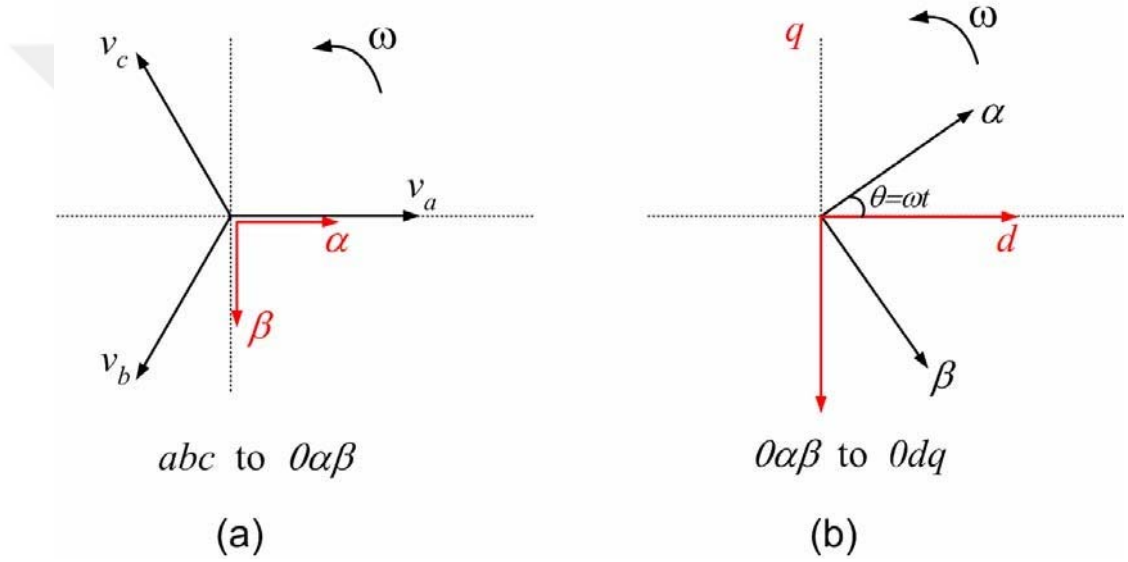


Figure A.2: Phasor diagrams used in deriving transformation matrices.

Since transformation matrices are “orthogonal matrices”, such that they satisfy (A.14) and (A.15).

$$C_1^T C_1 = 1 \quad (\text{A.14})$$

$$C_2^T C_2 = 1 \quad (\text{A.15})$$

The transformation matrices are applied to both sides of (A.7) as in (A.16). These transformation matrices are also applied to right-hand side of (A.8) and left-hand side of (A.9) as in (A.16) and (A.17), respectively.

$$C_1 C_1 \begin{bmatrix} v_0 \\ v_d \\ v_q \\ i_0 \\ i_d \\ q \end{bmatrix} = \begin{bmatrix} L_{P+R} & 0 & 0 & 1 & 0 & 0 \\ 0 & L_{P+R} & 0 & 0 & 1 & 0 \\ 0 & 0 & L_{P+R} & 0 & 0 & 1 \\ 1 & 0 & 0 & -3C_p & 0 & 0 \\ 0 & 1 & 0 & 0 & -3C_p & 0 \\ 0 & 0 & 1 & 0 & 0 & -3C_p \end{bmatrix} \begin{bmatrix} i_{s0} \\ i_{sd} \\ i_{sq} \\ v_{c0} \\ v_{cd} \\ v_{cq} \end{bmatrix} \quad (\text{A.16})$$

$$v_{dc} = [M \sin(\omega t + \theta) \quad M \sin(\omega t + \theta - 120^\circ) \quad M \sin(\omega t + \theta - 240^\circ)] \begin{bmatrix} v_{c0} \\ v_{cd} \\ v_{cq} \end{bmatrix} \quad (\text{A.17})$$

$$C_1 C_2 \begin{bmatrix} i_o \\ i_d \\ i_q \end{bmatrix} = \begin{bmatrix} M \sin(\omega t + \theta) \\ M \sin(\omega t + \theta - 120^\circ) \\ M \sin(\omega t + \theta - 240^\circ) \end{bmatrix} [i_{dc}] \quad (\text{A.18})$$

Equations in (A.16) and (A.18) can be arranged as in (A.19) and (A.20) respectively.

$$\begin{bmatrix} v_0 \\ v_d \\ v_q \\ i_0 \\ i_d \\ q \end{bmatrix} = C_2^{-1} C_1^{-1} \begin{bmatrix} L_{P+R} & 0 & 0 & 1 & 0 & 0 \\ 0 & L_{P+R} & 0 & 0 & 1 & 0 \\ 0 & 0 & L_{P+R} & 0 & 0 & 1 \\ 1 & 0 & 0 & -3C_p & 0 & 0 \\ 0 & 1 & 0 & 0 & -3C_p & 0 \\ 0 & 0 & 1 & 0 & 0 & -3C_p \end{bmatrix} C_1 C_2 \begin{bmatrix} i_{s0} \\ i_{sd} \\ i_{sq} \\ v_{c0} \\ v_{cd} \\ v_{cq} \end{bmatrix} \quad (\text{A.19})$$

$$\begin{bmatrix} i_o \\ i_d \\ i_q \end{bmatrix} = C_2^{-1} C_1^{-1} \begin{bmatrix} M \sin(\omega t + \theta) \\ M \sin(\omega t + \theta - 120^\circ) \\ M \sin(\omega t + \theta - 240^\circ) \end{bmatrix} [i_{dc}] \quad (\text{A.20})$$

In applying transformation matrices, the effect of operator “ p ” should be noted as given in (A.21). After applying transformation matrices to (A.17), (A.19) and (A.20), expressions in 0dq-stationary frame are obtained and given in (A.22), (A.23) and (A.24).

$$(L_{p+R}) \cos \omega t = -\omega L \sin \omega t + R \cos \omega t \quad (\text{A.21})$$

$$\begin{bmatrix} v_0 \\ v_d \\ v_q \\ i_0 \\ i_d \\ i_q \end{bmatrix} = \begin{bmatrix} L_{P+R} & 0 & 0 & 1 & 0 & 0 \\ 0 & L_{P+R} & -\omega L & 0 & 1 & 0 \\ 0 & \omega L & L_{P+R} & 0 & 0 & 1 \\ 1 & 0 & 0 & -3C_P & 0 & 0 \\ 0 & 1 & 0 & 0 & -3C_P & 3\omega C \\ 0 & 0 & 1 & 0 & -3\omega C & -3C_P \end{bmatrix} \begin{bmatrix} i_{s0} \\ i_{sd} \\ i_{sq} \\ v_{c0} \\ v_{cd} \\ v_{cq} \end{bmatrix} \quad (\text{A.22})$$

$$\begin{bmatrix} i_o \\ i_d \\ i_q \end{bmatrix} = \begin{bmatrix} 0 \\ \sqrt{\frac{3}{2}} M \sin \theta \\ -\sqrt{\frac{3}{2}} M \cos \theta \end{bmatrix} [i_{dc}] \quad (\text{A.23})$$

$$v_{dc} = \begin{bmatrix} 0 \\ \sqrt{\frac{3}{2}} M \sin \theta \\ -\sqrt{\frac{3}{2}} M \cos \theta \end{bmatrix} \begin{bmatrix} v_{c0} \\ v_{cd} \\ v_{cq} \end{bmatrix} \quad (\text{A.24})$$

So far, the differential equations in abc -rotating frame have been transformed into $0dq$ -stationary frame. From these equations, state-space representation of CSC can be derived. In this derivation zero sequence components are ignored since balanced system has already been assumed. Using (A.22), (A.23) and (A.24) and choosing state variables as i_{sd} , i_{sq} , v_{cd} , v_{cq} and i_{dc} state-space equations of CSC can be found as in (A.25).

$$\frac{d}{dt} \begin{bmatrix} i_{sd} \\ i_{sq} \\ v_{cd} \\ v_{cq} \\ i_{dc} \end{bmatrix} = \begin{bmatrix} -\frac{R}{L} & -\omega & -\frac{1}{L} & 0 & 0 \\ \omega & -\frac{R}{L} & 0 & -\frac{1}{L} & 0 \\ \frac{1}{3C} & 0 & 0 & -\omega & -\sqrt{\frac{3}{2}} \frac{M}{3C} \sin \theta \\ 0 & \frac{1}{3C} & \omega & 0 & -\sqrt{\frac{3}{2}} \frac{M}{3C} \cos \theta \\ 0 & 0 & \sqrt{\frac{3}{2}} \frac{M}{L_{dc}} \sin \theta & \sqrt{\frac{3}{2}} \frac{M}{L_{dc}} \cos \theta & -\frac{R_{dc}}{L_{dc}} \end{bmatrix} \begin{bmatrix} i_{sd} \\ i_{sq} \\ v_{cd} \\ v_{cq} \\ i_{dc} \end{bmatrix} + \begin{bmatrix} \frac{1}{L} & 0 \\ 0 & \frac{1}{L} \\ 0 & 0 \\ 0 & 0 \\ 0 & 0 \end{bmatrix} \begin{bmatrix} v_d \\ v_q \end{bmatrix} \quad (\text{A.25})$$

From the state-space representation of CSC STATCOM in (A.25), equivalent circuit in dq-stationary frame can be found as given in Fig.A.3. Advantage of the equivalent circuit in Fig.A.3 is that all quantities at supply frequency become dc-quantity in steady-state as shown in Fig.A.3b. This means that analysis of this circuit

is algebraic rather than vectorial.

The state space representation of CSC based STATCOM in (A.25) has the standard form given in (A.26).

$$\dot{x} = Ax + Bu \quad (A.26)$$

where x is the state vector
 (5×1) A is the constant
matrix (5×5) B is the
constant matrix (5×2)
 u is the input vector (2×1)

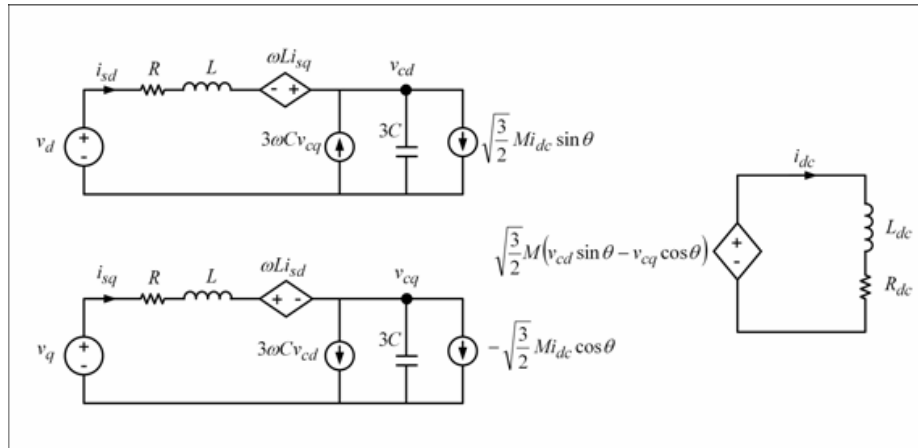
Supply voltages are given as in the form of input vector in (A.25). They have been defined for abc-rotating frame in (A.1). Applying transformation matrices to (A.1) yields the input vector u as in (A.27).

$$\begin{bmatrix} v_o \\ v_d \\ v_q \end{bmatrix} = C_2^{-1} C_1^{-1} \begin{bmatrix} v_R \\ v_S \\ v_T \end{bmatrix} = \begin{bmatrix} 0 \\ \sqrt{\frac{3}{2}} V \\ 0 \end{bmatrix} \quad (A.27)$$

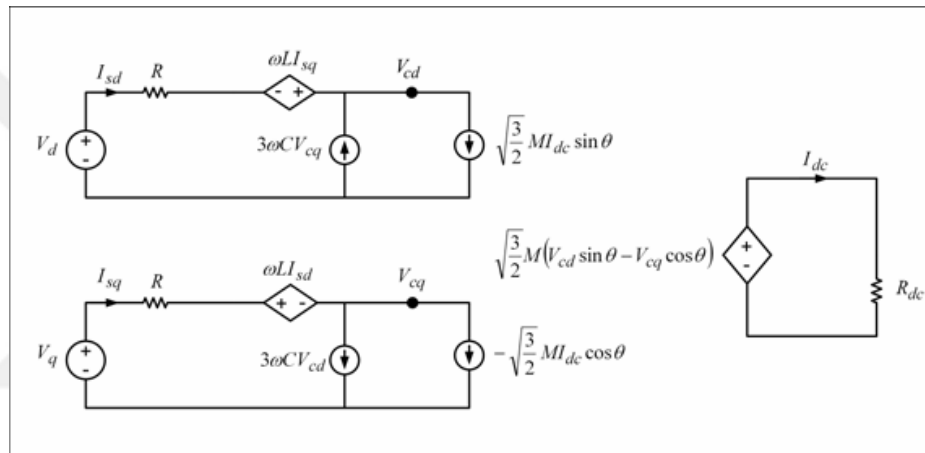
From the state space equations given in (A.25) and (A.26), steady-state expressions can be found by equating $dx/dt=0$ and solving for x as in (A.38).

$$x = A^{-1}Bu \quad (A.38)$$

Although expressions for state variables can be derived by solving (A.38) after a very long elementary matrix operations, the result will be too complicated. Therefore, rather than deriving the expressions, numerical solution can be easily found for the given system parameters by using computer programs, such as MATLAB.



(a) for transient-state



(b) for steady-state

Figure A.3: Equivalent circuit of CSC based STATCOM in dq-stationary frame.

Appendix-B: Calculations of K, J and N matrices

These calculation has been solved by using mat lab to get the desired gain matrices as following:

A=[-0.5 -75 0 0 0;0 -150 314 500 0;0 -314 -150 0 500;0 -2500 0 0 314;0 0 -2500 -314
0]

A =

```
1.0e+03 *  
-0.0005  -0.0750    0         0         0  
0        -0.1500   0.3140   0.5000   0  
0        -0.3140  -0.1500   0         0.5000  
0        -2.5000   0         0         0.3140  
0         0        -2.5000  -0.3140   0
```

B=[0 0;0 0;2500 0;0 2500]

B =

```
0    0  
0    0  
0    0  
2500 0  
0    2500
```

$$C=[1\ 0\ 0\ 0\ 0;0\ 0\ 1\ 0\ 0]$$

$$C =$$

$$\begin{bmatrix} 1 & 0 & 0 & 0 & 0 \\ 0 & 0 & 1 & 0 & 0 \end{bmatrix}$$

$$F=[0;-500;0;0;0]$$

$$F =$$

$$\begin{bmatrix} 0 \\ -500 \\ 0 \\ 0 \\ 0 \end{bmatrix}$$

$$p=[-99;-499;-289;-389;-399];$$

$$K=\text{place}(A,B,p)$$

$$K =$$

$$\begin{bmatrix} -0.1218 & -1.0121 & 0.1255 & 0.2553 & 0.2572 \\ -0.0185 & -0.1379 & -1.0051 & -0.2395 & 0.2945 \end{bmatrix}$$

$$j=(C*(-(A-B*K)^{-1}*B))^{-1}$$

j =

-0.1227 0.0046

-0.0186 0.1548

$$N = ((C * (-A + B * K)^{-1} * B))^{-1} * (C * (-A + B * K)^{-1} * F)$$

N =

-0.2553

0.1139

CURRICULUM VITAE

PERSONAL INFORMATION

Name, Surname : Mahmood ABED
Nationality : Iraqi
Date and Place of Birth : 1 September 1982, Iraq- Nineveh
Marital Status : Single
Phone : +90 5347205301
Email : wordk40@yahoo.com

EDUCATION

High School : AL-Sharqiya Secondary School, 2001.
Undergraduate : Technical College of Mosul / Electrical Power
Technology Engineering Department, 2005.

WORK EXPERIENCE

Year : 2012- Present
Place : Iraqi Ministry of Electricity/ Energy Distribution Office

FOREIGN LANGUAGE

English